A Method to Estimate Canal Leakage to the Biscayne Aquifer, Dade County, Florida

U.S. Geological Survey
Water-Resources Investigations Report 90-4135

Prepared in cooperation with the
South Florida Water Management District and
Metro-Dade Environmental Resources Management

A Method to Estimate Canal Leakage to the Biscayne Aquifer, Dade County, Florida

By David A. Chin

U.S. GEOLOGICAL SURVEY
Water-Resources Investigations Report 90–4135

Prepared in cooperation with the
SOUTH FLORIDA WATER MANAGEMENT DISTRICT and
METRO-DADE ENVIRONMENTAL RESOURCES MANAGEMENT

Tallahassee, Florida
1990

U.S. DEPARTMENT OF THE INTERIOR
MANUEL LUJAN, JR., Secretary

U.S. GEOLOGICAL SURVEY
Dallas L. Peck, Director

Use of brand names in this report is for identification purposes only and does not constitute endorsement by the U.S. Geological Survey.

For additional information
write to:

District Chief
U.S. Geological Survey
Suite 3015
227 North Bronough Street
Tallahassee, Florida 32301

Copies of this report can
be purchased from:

U.S. Geological Survey
Books and Open-File Reports
Federal Center, Building 810
Box 25425
Denver, Colorado 80225

CONTENTS

FIGURES

TABLES

ABBREVIATIONS AND CONVERSION FACTORS

The inch-pound units used in this report may be converted to metric (International System) units by the following factors:

Multiply inch pound unit	By	To obtain metric unit
inch (in.)	25.4	millimeter (mm)
foot (ft)	0.3048	meter (m)
foot per second (ft/s)	0.3048	meter per second (m/s)
foot per day (ft/d)	0.3048	meter per day (m/d)
square foot (ft^2)	0.09294	square meter (m^2)
foot squared per day (ft^2/d)	0.09290	meter squared per day (m^2/d)
mile (mi)	1.609	kilometer (km)
cubic foot per second (ft^3/s)	0.028317	cubic meter per second (m^3/s)
cubic foot per second per lineal foot [$(ft^3/s)/ft$)]	0.0176	cubic meter per second per lineal meter [$(m^3/s)/m$]
cubic foot per second per mile [$(ft^3/s)/mi$]	0.01760	cubic meter per second per kilometer [$(m^3/s)/km$]
cubic foot per second per mile per foot [$(ft^3/s)/mi/ft$]	0.05773	cubic meter per second per kilometer per meter [$(m^3/s)/km/m$]

Sea level: In this report "sea level" refers to the National Geodetic Vertical Datum of 1929 (NGVD of 1929)—a geodetic datum derived from a general adjustment of the first-order level nets of both the United States and Canada, formerly called "Sea Level Datum of 1929."

Additional abbreviations

AVM = acoustic velocity meter
kHz = kilohertz

A Method to Estimate Canal Leakage to the Biscayne aquifer, Dade County, Florida

By David A. Chin

ABSTRACT

The leakage characteristics of channels that partially penetrate the Biscayne aquifer and have reduced bed permeability were studied. Leakage characteristics were described in terms of a reach transmissivity—defined as the volume flow rate out of the channel per unit length of the channel per unit drawdown, where drawdown is defined as the difference in altitude between the water surface in the canal and the water table in the adjacent aquifer. A theoretical expression was developed to relate the reach transmissivity to the transmissivity of the formation, mean channel width, distance of drawdown measurement from the channel centerline, ratio of drawdowns on both sides of the channel, and local reach transmissivity associated with reduced bed permeability. This theoretical expression was verified using a fine-scale numerical model, which gave accurate results when drawdowns were measured beyond 10 aquifer depths from the side of the channel. Using the theoretical formulation, it is shown that the reach transmissivity employed in regional ground-water models, which are based on average drawdowns within a cell, depends on the size of the cell as well as the transmissivity of the formation, channel width, and local reach transmissivity due to reduced bed permeability.

The theoretical reach transmissivity function was compared with field measurements at L-31N Canal and Snapper Creek Extension Canal in Dade County, Florida. Analyses of the data for both canals showed good agreement between the estimated and measured reach transmissivities. At L-31N Canal, field measurements indicated that the local reach transmissivity was relatively uniform over a 2-mile reach of the channel (averaging 630 cubic feet per second per mile per foot), and the formation transmissivity was 1.8×10^6 feet squared per day. At Snapper Creek Extension Canal, an approximate analysis was necessary due to the inability of the acoustic velocity meter to measure very low water velocities in the channel. Assuming an aquifer transmissivity of 1×10^6 feet squared per day, drawdown measurements indicated that the local reach transmissivity was about 400 cubic feet per second per mile per foot. The theoretical relation, combined with the local reach transmissivity and formation transmissivity, was sufficient to predict the leakage out of L-31N Canal and Snapper Creek Extension Canal for any drawdown scenario.

INTRODUCTION

The canal system of south Florida performs many useful functions, including rapid removal of excess water, recharge of the surficial aquifer system, of which the Biscayne aquifer is the most important unit, and maintenance of hydraulic barriers against saltwater intrusion and contaminant migration in ground water. Numerical models are commonly used to simulate the movement of water between these canals and the shallow aquifer as a result of various stresses on the hydrologic system. To apply these water-management models, a quantitative knowledge of leakage into and out of the canals is essential.

Previous research on the leakage characteristics of canals in south Florida were concerned mainly with canals adjacent to the water-conservation areas (Klein and Sherwood, 1961; Meyer, 1971; Leach and others, 1972; Swayze, 1987), and the derived relations generally were in the form of volume flow rate into the canal per unit length of the canal per unit head difference between the canal and adjacent water body. These studies did not consider the asymmetrical water-table distribution about the channel and cannot be generally applied to canals throughout south Florida. A formal theory and experimental protocol for obtaining the leakage parameters under asymmetrical drawdown scenarios is not currently available.

Low water velocities, which are prevalent in south Florida canals, usually limit the accuracy of leakage measurements. More accurate flow-measurement techniques are needed so that reliable leakage estimates can be made. For this reason, the U.S. Geological Survey, in cooperation with the South Florida Water Management District and Metro-Dade Environmental Resources Management, began an investigation in October 1987 to develop methods for quantifying water exchange between canals and aquifer. This report presents the results of that investigation.

Purpose and Scope

This report describes the development of a quantitative relation between canal leakage and canal and aquifer characteristics in Dade County, Fla. The report reviews previous research on canal-leakage relations and identifies

formulations that are appropriate for describing leakage from canals under asymmetrical drawdown conditions. The validity of the proposed formulation is then investigated at two canal sites by comparing a theoretical relation with that determined from measurements. The flow measurements in the canals were obtained using acoustic velocity meters, which are capable of accurately measuring most low velocity flows.

Previous Research

The relation between leakage from open channels and the channel and aquifer properties has been studied by several researchers, starting with Dachler (1936). Bouwer (1965; 1969; 1978) summarized much of the research on leakage from open channels and identified three basic conditions (fig. 1) under which leakage occurs. Condition A occurs when the channel is underlain by a highly permeable zone, condition B occurs when the channel is underlain by an impermeable zone, and condition C occurs when the channel is lined with a zone in which the hydraulic conductivity is significantly less than that of the aquifer.

Leakage relations for conditions A, B, and C were presented by Bouwer (1965) for several simplified aquifer hydraulic conductivity distributions. For conditions A and B, these leakage relations relate the leakage out of the channel to the difference between the channel stage and the water table (D_w) at some distance (L) from the centerline of the channel. The parameters of this relation are the channel surface width (W_s), channel water depth (H_w), side slope (α), channel bottom width (W_b), depth to permeable or impermeable zone (D_p or D_i), and the hydraulic conductivity of the aquifer (K). When condition C exists, the channel is hydraulically disconnected from the aquifer and the leakage relation relates the channel leakage to the channel stage, with the parameters being the channel geometry and the hydraulic characteristics of the channel lining. Of particular importance in condition C are the hydraulic conductivity of the lining (K_a) and the thickness of the lining (L_a). In this report, the difference between the channel stage and water table at any given location will be referred to as the "drawdown" (D_w). Whenever the water table is below the channel stage, the drawdown is positive.

The channels of interest in this study are similar to condition B (fig. 1), except the perimeter of the channel may be underlain by low permeability sediments that produce significant local head losses. This situation differs from that in condition C in that the potentiometric surface of the aquifer is above the bottom of the channel (no unsaturated zone beneath the channel). For condition B, Bouwer (1965) found that when the distance from the channel bottom to the impermeable zone (D_i) was less than three times the bottom width of the channel (W_b) and provided the drawdown was measured at a distance (L) of at least $10W_b$ from the center of the channel, the channel could be assumed to be a fully penetrating constant-head boundary, and the Dupuit-Forcheimer

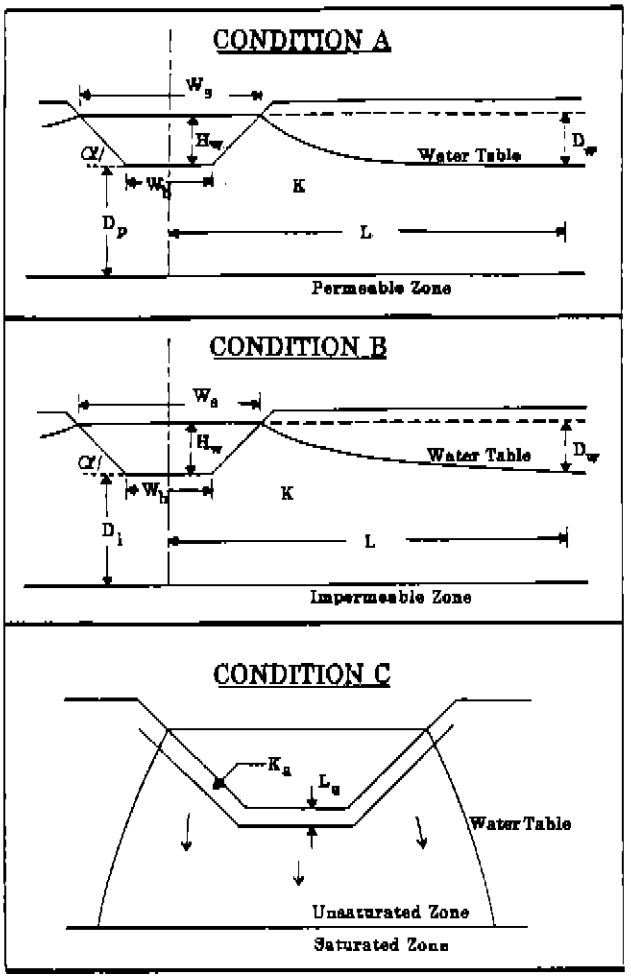

EXPLANATION

D_p = DEPTH TO PERMEABLE ZONE
D_i = DEPTH TO IMPERMEABLE ZONE
D_w = DRAWDOWN
H_w = DEPTH OF FLOW IN CHANNEL
K = HYDRAULIC CONDUCTIVITY OF AQUIFER
K_a = HYDRAULIC CONDUCTIVITY OF AQUIFER LINING
L = DISTANCE OF DRAWDOWN MEASUREMENT FROM CHANNEL LINING
L_a = THICKNESS OF CHANNEL LINING
W_b = BOTTOM WIDTH OF CHANNEL
W_s = TOP WIDTH OF CHANNEL
α = ANGLE THAT CHANNEL SIDES MAKE WITH HORIZONTAL

Figure 1. Previously identified leakage conditions.

(D-F) assumption could be used to estimate channel leakage. Under these conditions, leakage is directly proportional to drawdown, and the hydraulic conductivity distribution may be characterized simply by the transmissivity of the formation. This finding was reinforced by Ernst (1962) in a study of leakage from a channel into a two-layered soil, which showed that, based on the drawdown at a sufficient distance

from the channel, leakage was controlled primarily by the transmissivity. Bouwer (1965) also reported for condition B that leakage from the channel bottom is minor compared with leakage from the sides. As a result, sediment found on the channel bottom may have little effect on the relation between channel leakage and drawdown in the aquifer.

The previously discussed results were determined for trapezoidal channels. For channels of different shape, but with the same top width (W_s) and water depth (H_w), leakage relations do not change significantly with channel shape (Bouwer, 1965), provided the depth to the impermeable zone (D_i) is relatively small. The analytical results, presented by Bouwer (1969), can be summarized by the following equation,

$$Q = \Gamma D_w, \qquad (1)$$

where

Q is leakage out of the channel [$(L^3/T)/L$];

Γ is reach transmissivity [$(L^3/T)/L/L$]; and

D_w is drawdown at a particular distance from the channel [L].

The reach transmissivity (Γ) is the proportionality factor relating the leakage out of the canal to the drawdown at a given distance away from the channel. Γ is a function of both the aquifer and channel characteristics. The magnitude of Γ depends on the location where D_w is measured and may depend on D_w. In cases where the D-F assumption is valid, Γ will be independent of D_w. Equation 1 was previously used in several leakage models (Morel-Seytoux, 1975; Morel-Seytoux and Daly, 1975; Flug and others, 1980), and the parameter Γ was generally assumed to be constant. According to the results in Dachler (1936), this assumption probably is valid if D_w is measured at a distance from the channel that is significantly greater than L_o, where

$$L_o = \frac{W_s + H_w + D_i}{2}. \qquad (2)$$

Field verification of equation 1 was attempted by Morel-Seytoux and others (1979) for an 81-mile reach of the South Platte River between Balzac and Julesburg in northeastern Colorado. Leakage from the river was estimated from changes in discharge, and the reach transmissivity (Γ) was determined from measured drawdowns using equation 1. The reach transmissivity was also determined independently in that study using the formula,

$$\Gamma = \frac{T}{e} \frac{\left(\frac{W_p}{2} + e\right)}{5\,W_p + \frac{e}{2}}, \qquad (3)$$

where

T is transmissivity of the aquifer;

L is distance from the channel centerline to where drawdown is measured;

e is saturated thickness of the aquifer; and

W_p is wetted perimeter of the channel.

Results obtained using equation 3 are similar to those using the D-F assumption for a clean channel. In the Colorado field study, leakage predictions exceeded observations by an average of about 50 percent. This degree of agreement is impressive, considering the accuracy with which transmissivities and leakage losses were estimated. Mishra and Seth (1988) derived a theoretical expression describing leakage from a channel of large width, where $W_s > 4D_i$. These dimensions are not characteristic of many channels; however, they conclude that if D_w is measured beyond $0.5D_i$ from the channel, then Γ is independent of D_w.

Models of stream-aquifer systems can be analytical or numerical. Analytical models are typically used in simplified geologic formations and relate the channel leakage to aquifer drawdown by the reach transmissivity according to equation 1 (for example, Morel-Seytoux and Daly, 1975). Other analytical models treat the stream as a fully penetrating constant-head boundary (Jenkins, 1968; Hantush and Mariño, 1989). The former approach is more general, although under some circumstances both methods are applicable. Numerical models that simulate channels generally express the channel leakage (or net flux) into a cell block containing a channel as being equal to the product of a user-defined reach transmissivity and the difference between the channel stage and head in the cell, which is usually assumed to describe aquifer conditions immediately adjacent to the channel (MacVicar and others, 1984; McDonald and Harbaugh, 1988). It is important to remember that the reach transmissivity depends on the location in which the drawdown is measured and may vary with model approach.

Previous studies of channel leakage assumed drawdowns adjacent to the channel were either symmetrical to the channel, or the channel was wide enough so that leakage relations on both sides of the channel were independent (Mishra and Seth, 1988). The role of reduced bed permeability (caused by the formation of a semipermeable channel lining) on these leakage scenarios had not been studied previously.

DEVELOPMENT OF A METHOD TO ESTIMATE CANAL LEAKAGE

Analytical Model

Based on the results of Bouwer (1965), if the depth of the aquifer beneath the channel is less than 3 channel bottom widths, and the drawdown is known at a distance beyond 10 channel widths away from the centerline of the channel, then the D-F assumption can be used to determine the reach transmissivity. In a more general form, this result indicates that the D-F assumption is applicable in determining the reach transmissivity at distances on the order of (and beyond) four aquifer depths away from the channel.

Although equations from Bouwer (1965) were applied to symmetrical drawdown cases, the D-F assumption may also be valid for the asymmetrical drawdown case (fig. 2). Asymmetrical drawdowns often occur because of unequal stresses on the aquifer along the sides of the channel (for example, heavy pumping on one side of the channel). If leakage out of the channel per unit channel length is given by Q_c, and the seepage out of the left and right boundaries per unit channel length is given by Q_L and Q_R, then these values are related by

$$Q_c = Q_L + Q_R. \quad (4)$$

If the transmissivity of the aquifer is T, the leakage out of the channel can be estimated by

$$Q_c = \frac{T D_L}{(L - \overline{W}/2)} + \frac{T D_R}{(L - \overline{W}/2)}, \quad (5)$$

in which L is the distance from the center of the channel to where D_L and D_R are measured, and $\overline{W}$ is the mean width of the channel.

Equation 5 is based on the D-F assumption and implicitly assumes that L exceeds four aquifer depths. Another assumption is that the drawdown on one side of the channel does not significantly affect flow out of the other side of the channel. This wide-channel assumption is subsequently verified in two cases: (1) where the perimeter of the channel is not underlain by sediments with lower permeability, and (2) where the perimeter of the channel is underlain by relatively low permeability sediments.

Case 1

In case 1, where the channel is not separated from the aquifer by less-permeable bed materials, the reach transmissivity (T_r), relative to the drawdown on the right side of the channel (D_R), can be defined by

$$Q_c = T_r D_R. \quad (6)$$

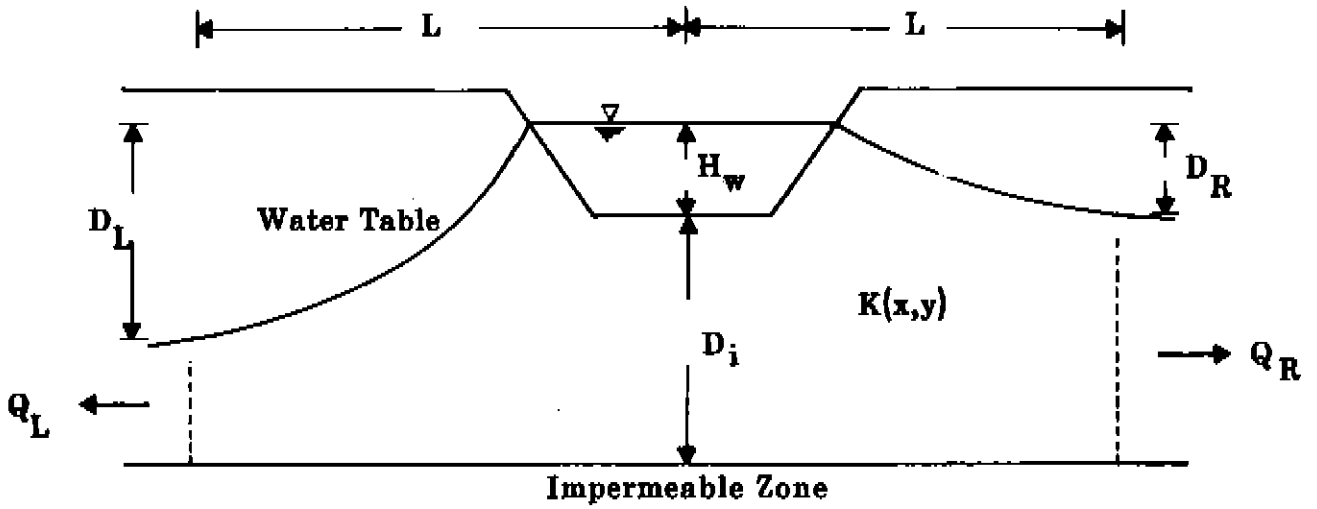

EXPLANATION

D_i = DEPTH TO IMPERMEABLE ZONE
D_R = DRAWDOWN ON RIGHT HAND SIDE OF CHANNEL
D_L = DRAWDOWN ON LEFT HAND SIDE OF CHANNEL
H_w = DEPTH OF FLOW IN CHANNEL
K = HYDRAULIC CONDUCTIVITY OF AQUIFER
L = DISTANCE FROM CHANNEL TO DRAWDOWN MEASUREMENT
Q_L = FLOW AWAY FROM CHANNEL ON LEFT HAND SIDE
Q_R = FLOW AWAY FROM CHANNEL ON RIGHT HAND SIDE

Figure 2. Asymmetrical leakage condition.

Combining equations 5 and 6 yields

$$\Gamma_r = \frac{T}{(L - \bar{W}/2)} \left(1 + \frac{D_L}{D_R}\right) . \quad (7)$$

If the drawdown is symmetrical ($D_L = D_R$), then the symmetrical-drawdown reach transmissivity (Γ_o) can be derived from equation 7 as

$$\Gamma_o = \frac{2T}{(L - \bar{W}/2)} . \quad (8)$$

Equations 7 and 8 can then be combined to yield

$$\Gamma_r = \frac{\Gamma_o}{2} \left(1 + \frac{D_L}{D_R}\right) , \quad (9)$$

which reflects the condition that when $D_L = -D_R$, zero net leakage occurs out of the channel. A negative drawdown indicates that the water table is above the canal stage, and the ground water is flowing toward the channel.

Case 2

In case 2, the channel is separated from the aquifer by less-permeable bed materials. As less-permeable materials start to accumulate on the channel bed, the increased resistance to flow causes leakage to decrease at areas of greatest sediment accumulation and increase at areas of least accumulation. An increased leakage rate in a channel with suspended sediments generally results in an increased sediment accumulation rate. Thus, as leakage increases around the perimeter of the channel, it is moderated by a higher sediment accumulation rate and tends to increase at other more permeable parts. This process continues indefinitely to maintain an approximate constant-head loss across the semipermeable perimeter. Denoting the head loss across the semipermeable layer by Δh, a local reach transmissivity (Γ_L) associated with the semipermeable channel lining can be defined. Leakage out of the channel is then given by

$$Q_c = \Gamma_L \Delta h. \quad (10)$$

There is also head loss associated with the transmissivity of the formation, with a reach transmissivity (Γ_r), such that

$$Q_c = \Gamma_r (D_R - \Delta h), \quad (11)$$

where Γ_r is the reach transmissivity of the channel in the absence of a semipermeable lining. An effective reach transmissivity (Γ_R) that includes the formation head loss as well as the head loss through the semipermeable channel lining can be defined by

$$Q_c = \Gamma_R D_R. \quad (12)$$

Combining equations 10 to 12 yields

$$\frac{1}{\Gamma_R} = \frac{1}{\Gamma_L} + \frac{1}{\Gamma_r} , \quad (13)$$

which shows the effective reach transmissivity as the harmonic mean of the local and formation reach transmissivities. If equation 9 is expressed for a semipermeable perimeter, then the formation reach transmissivity (Γ_r) is given by

$$\Gamma_r = \frac{\Gamma_o}{2} \left(1 + \frac{D_L - \Delta h}{D_R - \Delta h}\right) . \quad (14)$$

Combining equations 10 to 14 yields

$$\Gamma_R = \frac{\Gamma_L \Gamma_o}{2(\Gamma_L + \Gamma_o)} \left(1 + \frac{D_L}{D_R}\right) . \quad (15)$$

Numerical Model

Analytical, semianalytical, and analog models have been the primary approaches used to study canal leakage to the aquifer. Analytical and semianalytical models (Dachler, 1936; Harr, 1962; Dillon and Liggett, 1983; Mishra and Seth, 1988; Singh, 1989) generally are limited to simple geometries and aquifer characteristics. Analog models (Bouwer, 1965; Herbert, 1970) can simulate more complex geologies, but are expensive to construct and not easily modified. For this study, a small-scale ground-water flow model was used to simulate leakage from canals in response to aquifer drawdowns.

The finite-difference ground-water flow model (MODFLOW), developed by McDonald and Harbaugh (1988), can be used to explicitly model canal-aquifer interaction. The canal and impermeable layers are modeled using constant-head cells and no-flow cells, respectively. This model can use cells of varying sizes, so that in the vicinity of the canal where head gradients are large, smaller cell sizes can be used, and larger cell sizes can be used farther away from the canal. Different hydraulic conductivities may be assigned to each cell, allowing for simulation of complex hydrogeological conditions.

Conditions previously studied by Dachler (1936) and Bouwer (1965) were simulated and the results compared with those obtained using MODFLOW. Conditions A and B (fig. 1) were simulated to compare the leakage out of the trapezoidal channel with previous results. The grid and boundary conditions used in the MODFLOW simulations are shown in figure 3. The water within the channel was defined by constant-head cells. The water-table altitude at a distance $10W_b$ away from the channel centerline was also defined by constant-head cells. This formulation implicitly required that the streamlines be horizontal at the boundaries. The validity of this assumption was tested by comparing the predicted channel leakages with previously reported results. The locations of centers of the cells coincide exactly with the node locations in Bouwer's (1965) analog model. The model was run for varying values of D_w/W_b, and the seepage out of the canal constant-head cells was reported directly by MODFLOW. Results of these simulations are compared

with previously reported analytical results (Dachler, 1936) and analog results (Bouwer, 1965) in figure 4. Following the convention of Bouwer (1965), canal leakage is measured by the quantity I_s/K, where K is the hydraulic conductivity of the formation, and I_s, leakage per unit surface area of channel, is given by

$$I_s = \frac{Q}{W_s l}, \qquad (16)$$

where Q is the leakage, W_s is the surface width, and l is the canal reach length.

There is excellent agreement between the model results and the analytical and analog results as evidenced in figure 4. The greatest deviation between the results of Dachler (1936) and Bouwer (1965) occurs in condition B, when D_w/W_b is greater than about two, a scenario that is never found in south Florida.

The excellent agreement between the MODFLOW results and those previously reported indicates that the basic physics are being accurately simulated. Hence, MODFLOW can be confidently applied to cases of more complex geometry and geology.

Model Verification

A study was conducted to verify that the theory previously given (eq. 15) is applicable to real channels. MODFLOW was used to simulate leakage out of two major south Florida canals (L-31N and Snapper Creek Extension) and the resulting reach transmissivity compared with equation 15. The locations of the channel reaches investigated in this study along with the locations of the representative cross sections are shown in figure 5. Leakage from these canals supply water to adjacent well fields, and the drawdowns in the vicinity of the well fields are asymmetrical.

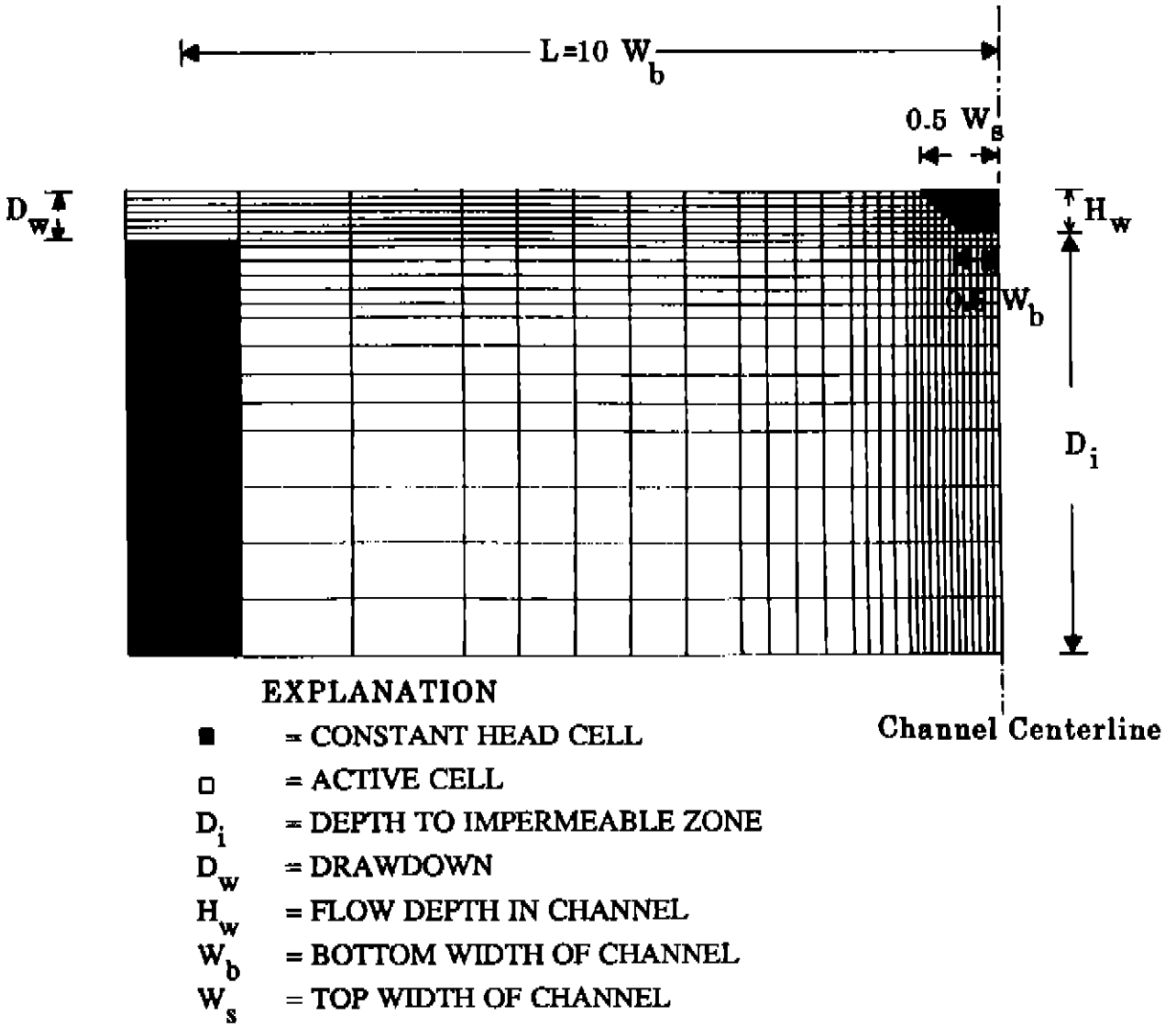

Figure 3. Grid and boundary conditions used in model verification.

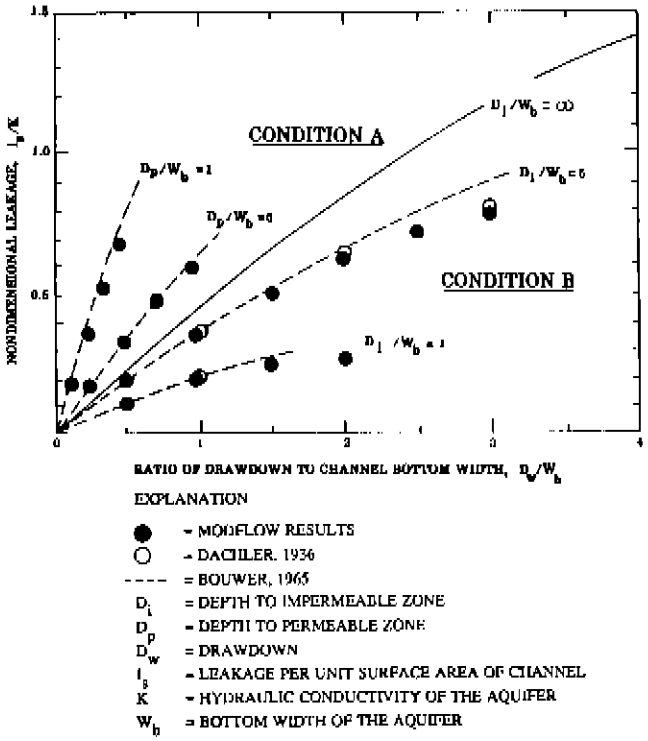

Figure 4. Plot showing verification of numerical model for conditions A and B.

L-31N Canal

A cross section of L-31N Canal is shown in figure 6. The approximate location of this cross section is shown in figure 5. This canal, located in Dade County, Fla., has a bank altitude about 8.0 feet above sea level, a bottom altitude about 12.0 feet below sea level, and a regulated canal stage about 3.5 feet above sea level. A sediment layer about 18-inches thick covers the canal bottom. The hydraulic conductivity of a core from this layer, which was measured using a permeameter, was 0.03 ft/d, indicating that the layer is effectively impermeable. However, the layer is apparently not present on the sides of the channel, which suggests most leakage probably is out of the sides.

The canal penetrates the Biscayne aquifer, which has a bottom altitude 52 feet below sea level at the canal site. The aquifer is about 55.5-feet thick and consists of two distinct geologic formations: the Miami Oolite and the Fort Thompson Formation (Klein and Hull, 1978). The hydraulic conductivities of the Miami Oolite and the Fort Thompson Formation are about 5,000 and 40,000 ft/d, respectively, although significant local variations from these values may exist (Fish and Stewart, 1990). The transmissivity at the canal site is about 1.2×10^6 ft^2/d (Klein and Hull, 1978). In this verification study, the hydraulic conductivities of the various formations at the canal site are assumed to be:

10 ft/d - Fill and organic deposits
4,500 ft/d - Miami Oolite
27,500 ft/d - Fort Thompson Formation

These values result in a transmissivity of about 1.2×10^6 ft^2/d. Although the hydraulic conductivities are not exactly known, it is important to recall that the reach transmissivity (eq. 15) depends only on the formation transmissivity and not on the exact hydraulic conductivity distribution. This assumption is subsequently verified.

The discretization of the canal and aquifer is shown in figure 7. Cells, 1-foot square, were used in the vicinity of the canal, with the cell size increasing geometrically away from the channel. Constant-head cells were used to define the interior of the channel, the bottom of the aquifer was defined by inactive cells, and the lateral boundaries (10 canal widths from the canal centerline) were specified as constant-head boundaries. Drawdowns on both sides of the channel were changed by varying the heads in these outer cells. Sedimentation around the perimeter of the channel was simulated by varying the hydraulic conductivity in the layer that surrounds the channel according to

$$Q_c = \frac{K P \Delta h}{\Delta s} \qquad (17)$$

and

$$Q_c = \Gamma_L \Delta h, \qquad (18)$$

where

Q_c is leakage out of the channel per unit channel length;
K is hydraulic conductivity of the low permeability sediment layer;
P is perimeter of the semipermeable layer;
Δh is head loss across the semipermeable layer;
Δs is thickness of the semipermeable layer; and
Γ_L is local reach transmissivity.

Combining equations 17 and 18 yields

$$\Gamma_L = \frac{K P}{\Delta s} . \qquad (19)$$

This equation is the basis for specifying the hydraulic conductivity of the semipermeable channel lining, based on given values of local reach transmissivity (Γ), wetted perimeter (P), and cell width (Δs).

Snapper Creek Extension Canal

A cross section of Snapper Creek Extension Canal is shown in figure 8. This channel has a bank altitude about 5 feet above sea level and a bottom altitude about 25 feet below sea level. The channel shape is deeper and narrower than that at L-31N Canal. On the basis of regulated stages from 1 to 3 feet above sea level, the width-to-depth ratio is about 2.9, whereas at L-31N Canal the ratio is 6.3. Snapper Creek Extension Canal has a layer of sediment deposits on the bottom with no apparent layer on the sides. The thickness of the sediment layer was not measured.

At the canal site, the bottom of the Biscayne aquifer is about 68 feet below sea level, and thus, when the canal stage is 2 feet, the saturated thickness of the aquifer is 70 feet. The aquifer primarily consists of fill, the Miami Oolite, and the Fort Thompson Formation (Labowski, 1988). The transmissivity of the overall formation is about 1×10^6 ft^2/d (Klein and Hull, 1978). Estimated hydraulic conductivities assigned to each formation, in accordance with typical values reported by Fish and Stewart (1990), are given below:

100 ft/d - Fill
1,000 ft/d - Miami Oolite
10,000 ft/d - Upper part of Fort Thompson Formation
27,500 ft/d - Lower part of Fort Thompson Formation

This hydraulic conductivity distribution corresponds to a transmissivity of 1×10^6 ft^2/d. Although the hydraulic conductivity in each formation is not exactly known, the reach transmissivity depends only on the formation transmissivity and is independent of the hydraulic conductivity distribution. This assumption is subsequently verified.

The discretization of the channel aquifer system is shown in figure 9. The cell size in the vicinity of the channel was 1-foot square, and it increased geometrically away from the channel. The channel interior was specified by constant-head cells, and the lateral boundaries of the simulation were specified by constant-head cells in which the centers were 10 channel widths from the channel

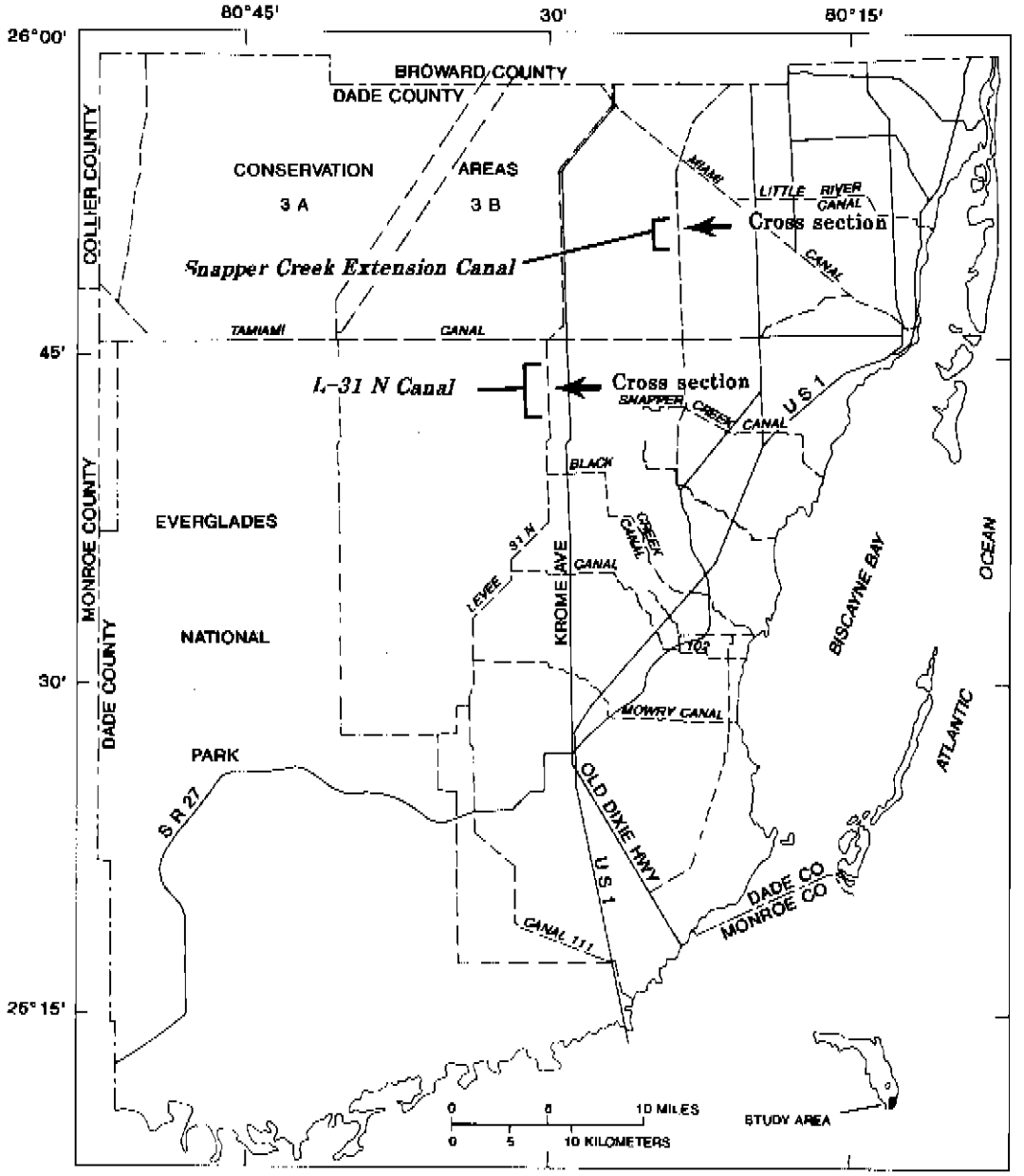

Figure 5. Location of the channels studied in Dade County.

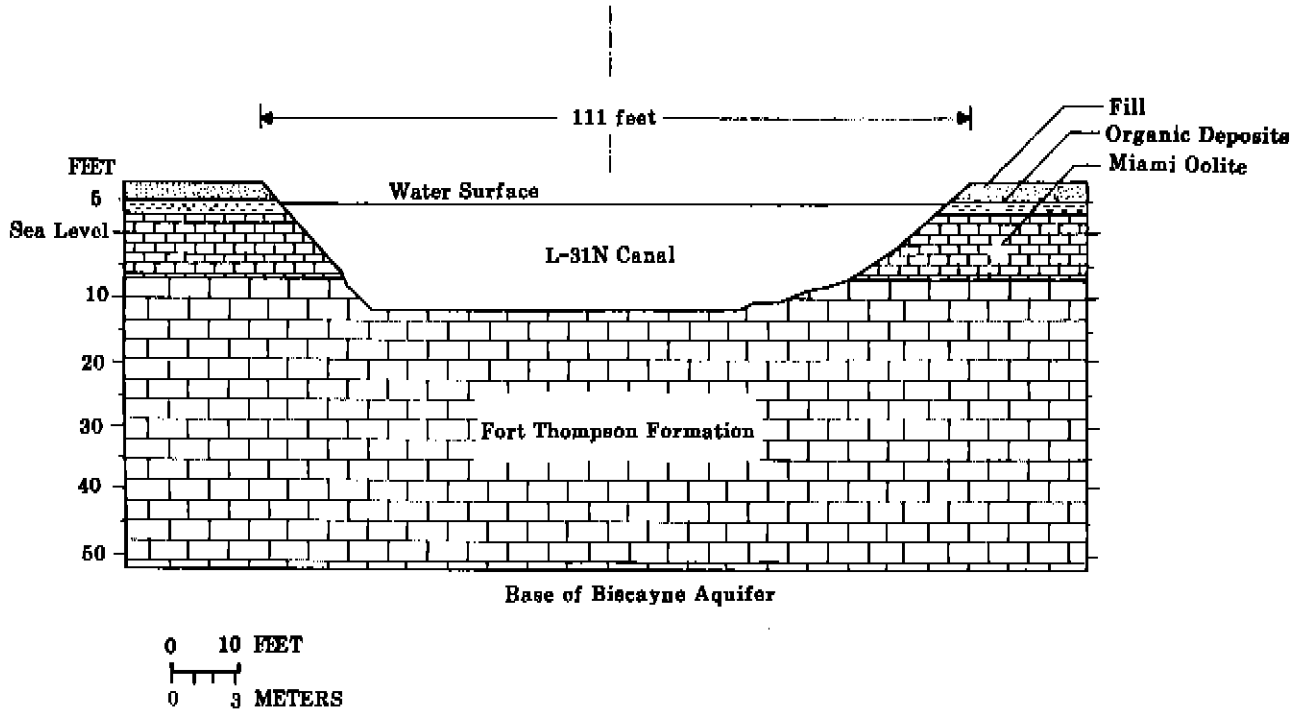

Figure 6. Typical cross section of L-31N Canal.

centerline. A semipermeable layer and the associated reach transmissivity were simulated using the same method previously described for L-31N Canal.

Results

As postulated earlier, if drawdowns are measured at locations that exceed four aquifer depths from the channel centerline, then the reach transmissivity (Γ_R), defined as the channel leakage per unit channel length per unit drawdown on the right, is given by equation 15. This equation can be expressed in the nondimensional form

$$\Gamma^* = \frac{\frac{\Gamma_L}{\Gamma_o}}{1 + \frac{\Gamma_L}{\Gamma_o}} . \qquad (20)$$

where Γ^* is the ratio of the actual reach transmissivity to the reach transmissivity of the channel open to the aquifer defined by equation 9. The reach transmissivity factor (Γ^*) is, therefore, given by

$$\Gamma^* = \frac{\Gamma_R}{\frac{\Gamma_o}{2}\left(1 + \frac{D_L}{D_R}\right)} . \qquad (21)$$

If this postulated theory is correct, then the leakage from both L-31N Canal and Snapper Creek Extension Canal obeys equation 20. On the basis of the transmissivity (T), average channel width (W), and distance to where drawdowns are measured (L), the value Γ_o for each channel can be calculated from equation 8. These results are given as follows:

Canal	Transmissivity, T (feet squared per day)	Distance from channel centerline, L (feet)	Mean channel width, $\overline{W}$ (feet)	Γ_o (cubic feet per second per mile per foot)
L-31N	1.2×10^6	556	88	286
Snapper Creek Extension	1.0×10^6	580	49	220

Using the numerical model, the leakage out of each channel was determined for various local reach transmissivities (Γ_L) and drawdown ratios (D_L/D_R). The simulated leakages were normalized into a reach transmissivity factor according to equations 12 and 21. Results are compared with the proposed theory in figure 10. The agreement between the theory and numerical results is good. The formations in the aquifer varied from stratified (S) conditions to equivalent unstratified (U) conditions with the same transmissivity. Also, the channels were simulated with either permeable (P) or impermeable (I) layers covering the channel bottom.

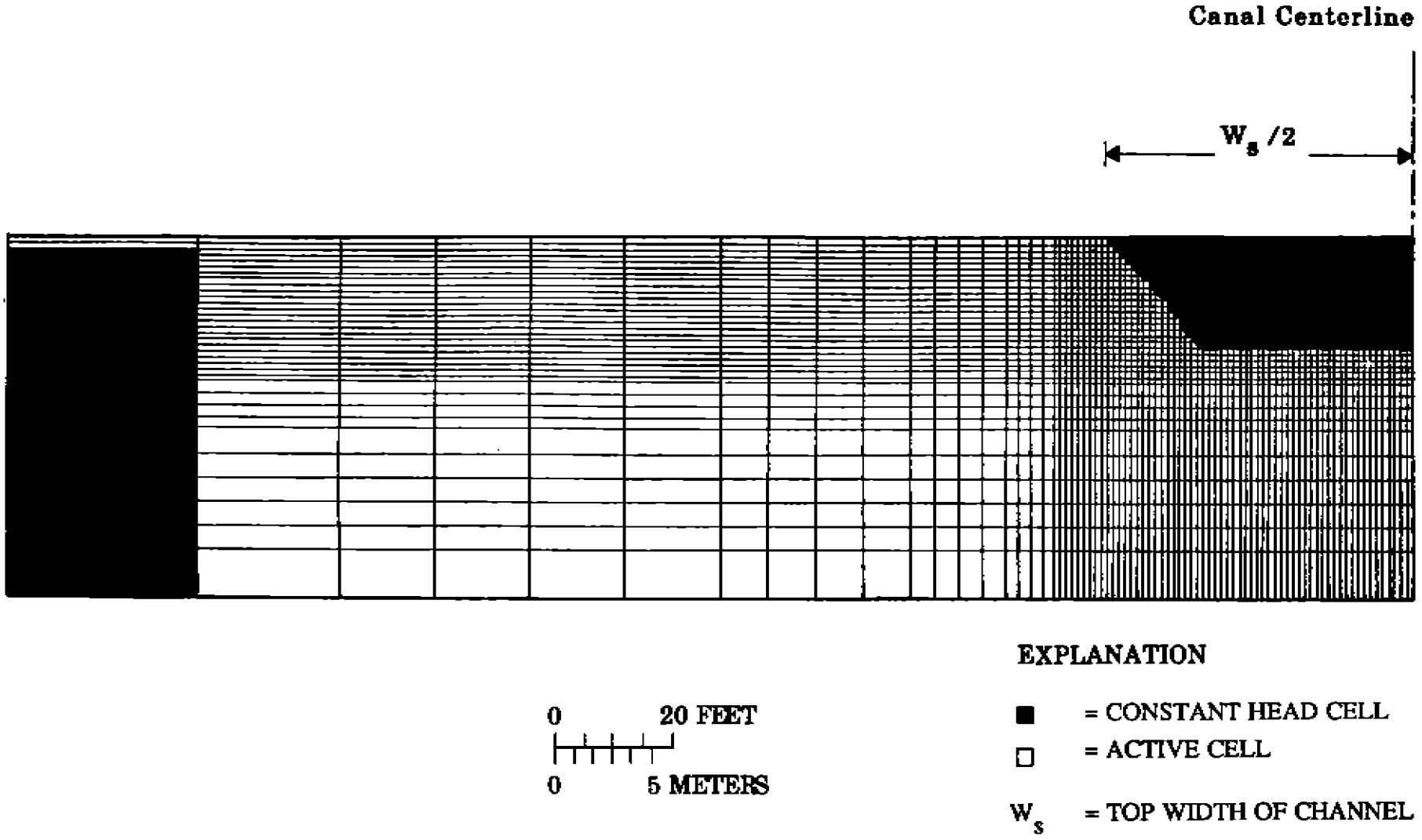

Figure 7. Numerical discretization of L-31N Canal transect.

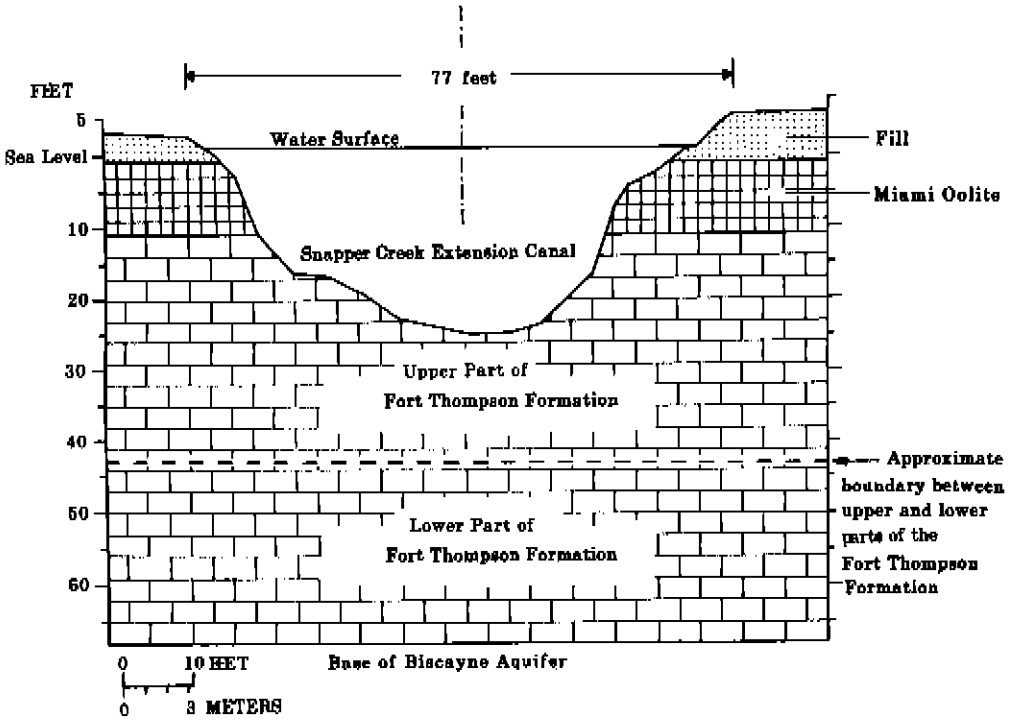

Figure 8. Typical cross section of Snapper Creek Extension Canal.

The good agreement between the numerical model and theory is relatively insensitive to the hydraulic conductivity distribution and impermeable bottom layer (fig. 10). These results support the assumption that beyond four aquifer depths from the channel centerline, leakage depends only on the transmissivity and not on the hydraulic conductivity distribution. Furthermore, the proposed theory remains valid even when the channel bottom is completely impermeable and only the sides underlain by a semipermeable layer. In this case, which is typical of both channels being studied, the local reach transmissivity is determined by equation 19, where the channel sides are used instead of the entire perimeter. For each value of the local reach transmissivity, the drawdown ratio (D_L/D_R) was varied within the range ±11, and the reach transmissivity showed no significant variation (fig. 10). Hence, the functional relation between the reach transmissivity (Γ_R) and the drawdown ratio (D_L/D_R) is accurately described by equation 15.

The above analysis has demonstrated the accuracy of the proposed theory for drawdowns measured at distances of 12.8 and 12.6 aquifer depths from L-31N Canal and Snapper Creek Extension Canal, respectively. An important question is how the accuracy of the proposed theory varies as the location of the drawdown measurement approaches the channel. To investigate this condition, the above analysis was repeated for distances ranging between 12.8 and 0.12 aquifer depths from the sides of the channels. Results are shown in figure 11 for values of D_L/D_R in the range ±11. As the distance from the channel decreases, the amount of scatter in the results increases, primarily because channel leakage becomes more sensitive to near-channel conditions, and the D-F assumption becomes less valid. However, beyond 9.5 aquifer depths from the side of the channel, all results are within 10 percent of the theoretical prediction, and beyond 5 aquifer depths, they are within 20 percent.

All the results discussed above indicate that the proposed formulation for the reach transmissivity provides an excellent description of the leakage characteristics of the channels investigated. Furthermore, because of its nondimensional nature, the proposed formulation may be widely applicable.

Applications in Regional Numerical Models

In regional numerical ground-water models, the hydraulic head in any cell is often assumed to be equal to the average head in that cell. Jorgensen and others (1989) discussed the importance of analyzing intracell flows in specifying source and sink terms used in regional ground-water models. Specifically, they reported some error is almost always introduced in the computed leakage if the cell-averaged head is used as the head just below the stream, and the difference between this head and the canal stage is multiplied by the local reach transmissivity to obtain the leakage. To circumvent this problem, a new formulation is proposed.

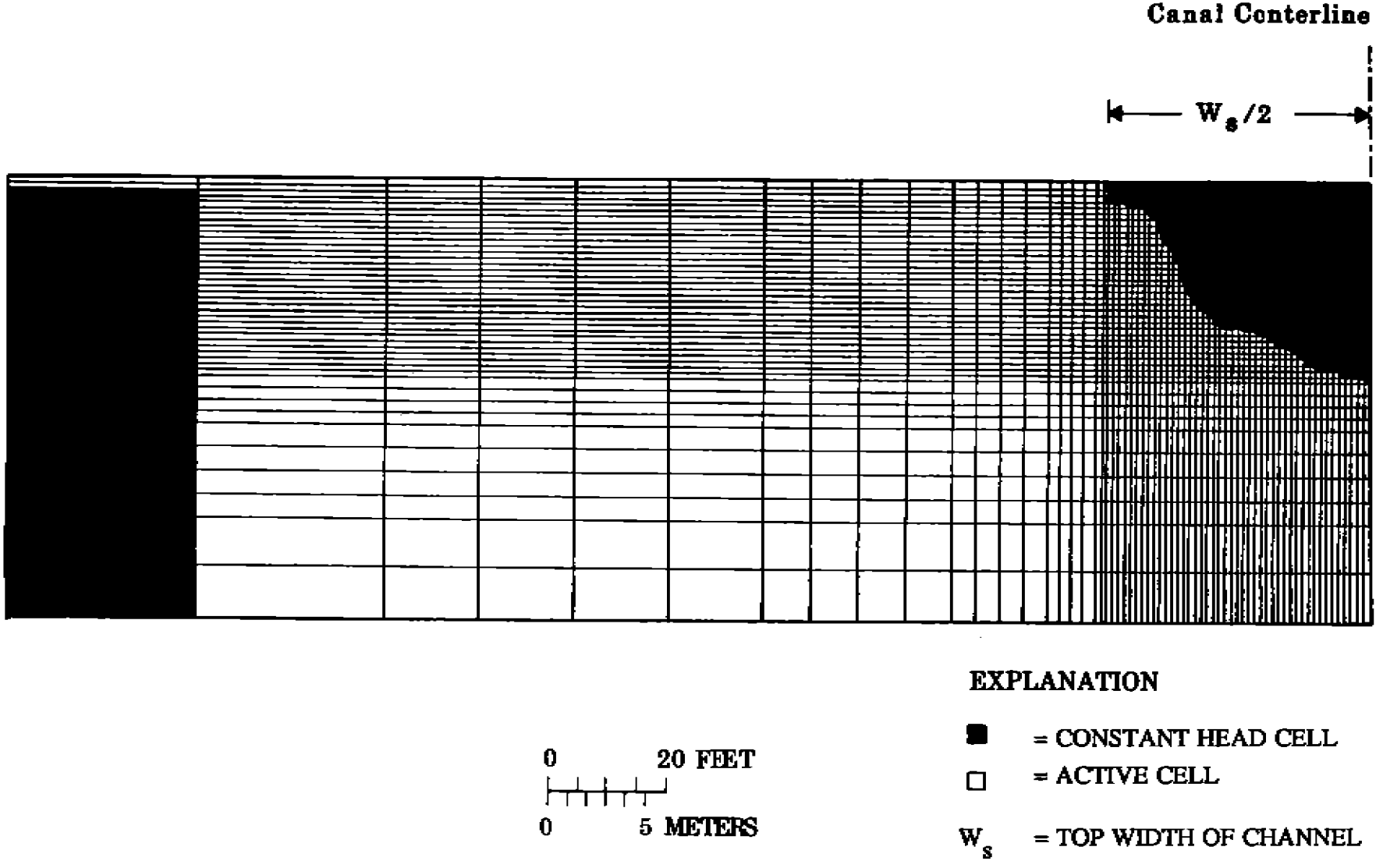

Figure 9. Numerical discretization of Snapper Creek Extension Canal transect.

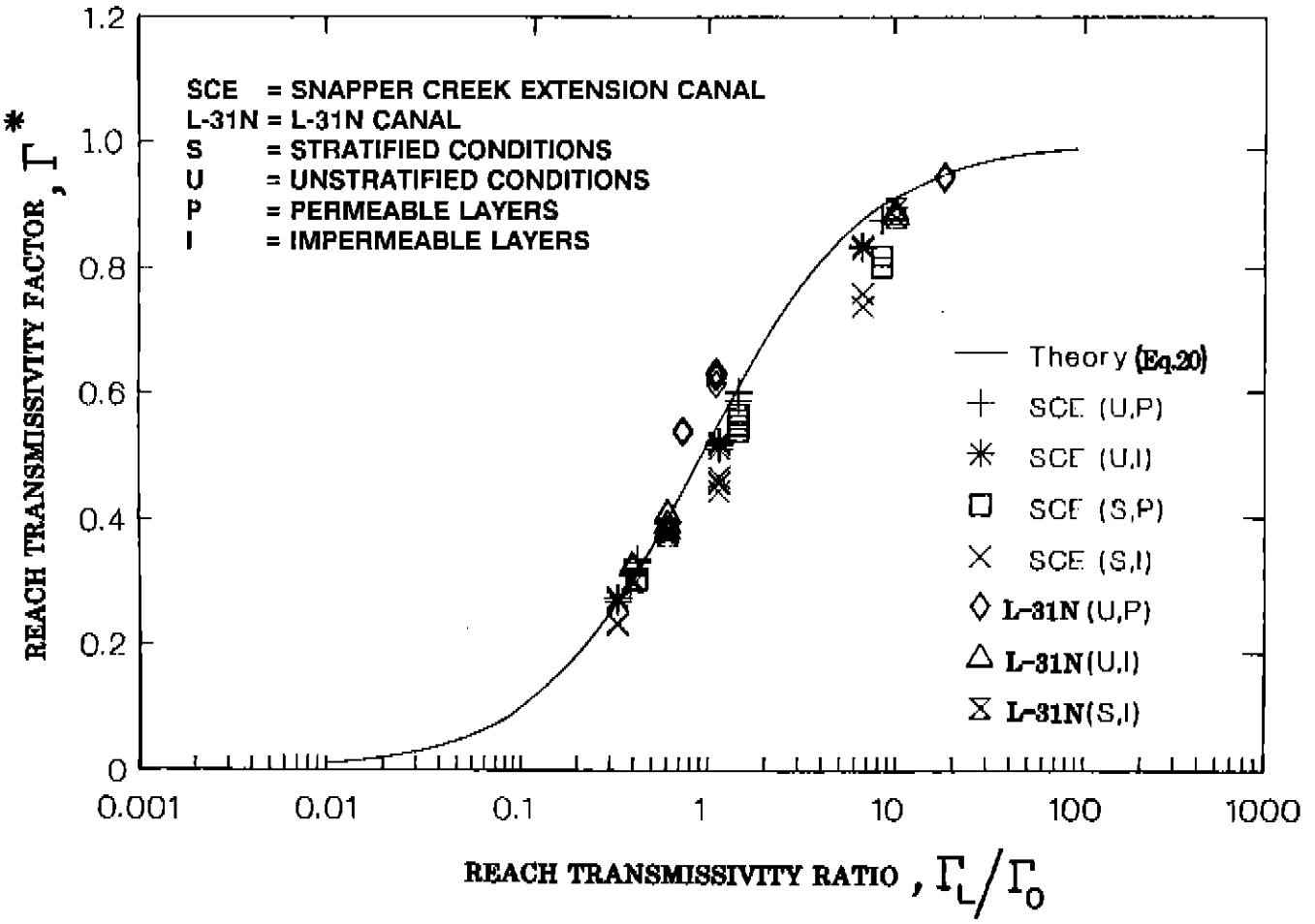

Figure 10. Relation between reach transmissivity factor and reach transmissivity ratio.

A typical intracell-head distribution is shown in figure 12. In this case, the channel is in the center of the cell that is Δx wide. The drawdown adjacent to the channel is Δh, and the drawdowns on the left and right sides of the cell are D_L and D_R, respectively. Assuming these conditions are uniform along the channel, then the mean drawdown in the cell ($\bar{D}$) is given by

$$\bar{D} = (D_L + D_R)\left[\frac{1 - \frac{W}{\Delta x}}{4}\right] + \Delta h\left[\frac{1 + \frac{W}{\Delta x}}{2}\right]. \quad (22)$$

After some rearrangement, combining the fundamental leakage equation (eq. 15) with equations 18 and 22 gives

$$Q_c = \left\{\frac{2\Gamma_L}{\frac{\Gamma_L}{\Gamma_o}\left(1 - \frac{W}{\Delta x}\right) + 2}\right\}\bar{D}, \quad (23)$$

where Q_c is the leakage out of the channel. If a reach transmissivity appropriate for the cell (Γ_c) on the basis of average drawdown in the cell ($\bar{D}$) is defined by

$$\Gamma_c = \frac{Q_c}{\bar{D}}, \quad (24)$$

then combining equations 23 and 24 yields the following expression for the cell reach transmissivity in terms of the local and formation reach transmissivities,

$$\Gamma_c = \frac{2\Gamma_L}{\frac{\Gamma_L}{\Gamma_o}\left(1 - \frac{W}{\Delta x}\right) + 2}. \quad (25)$$

The value Γ_c depends on the size of the cell by way of its dependence on Γ_o, which according to equation 8, is given by

$$\Gamma_o = \frac{4T}{\Delta x - W}, \quad (26)$$

where T is the transmissivity of the formation. Also, Γ_L is independent of the cell size. In combining equations 25 and 26, it is apparent that as the cell size (Δx) increases, the cell reach transmissivity decreases according to the relation

$$\Gamma_c = \frac{8T\Gamma_L\Delta x}{\Gamma_L(\Delta x - W)^2 + 8T\Delta x}. \quad (27)$$

In a regional flow model using cell-averaged heads, T, Γ_L, Δx, and W must be known and equation 27 used to find Γ_c, which is the leakage parameter in almost all regional flow models.

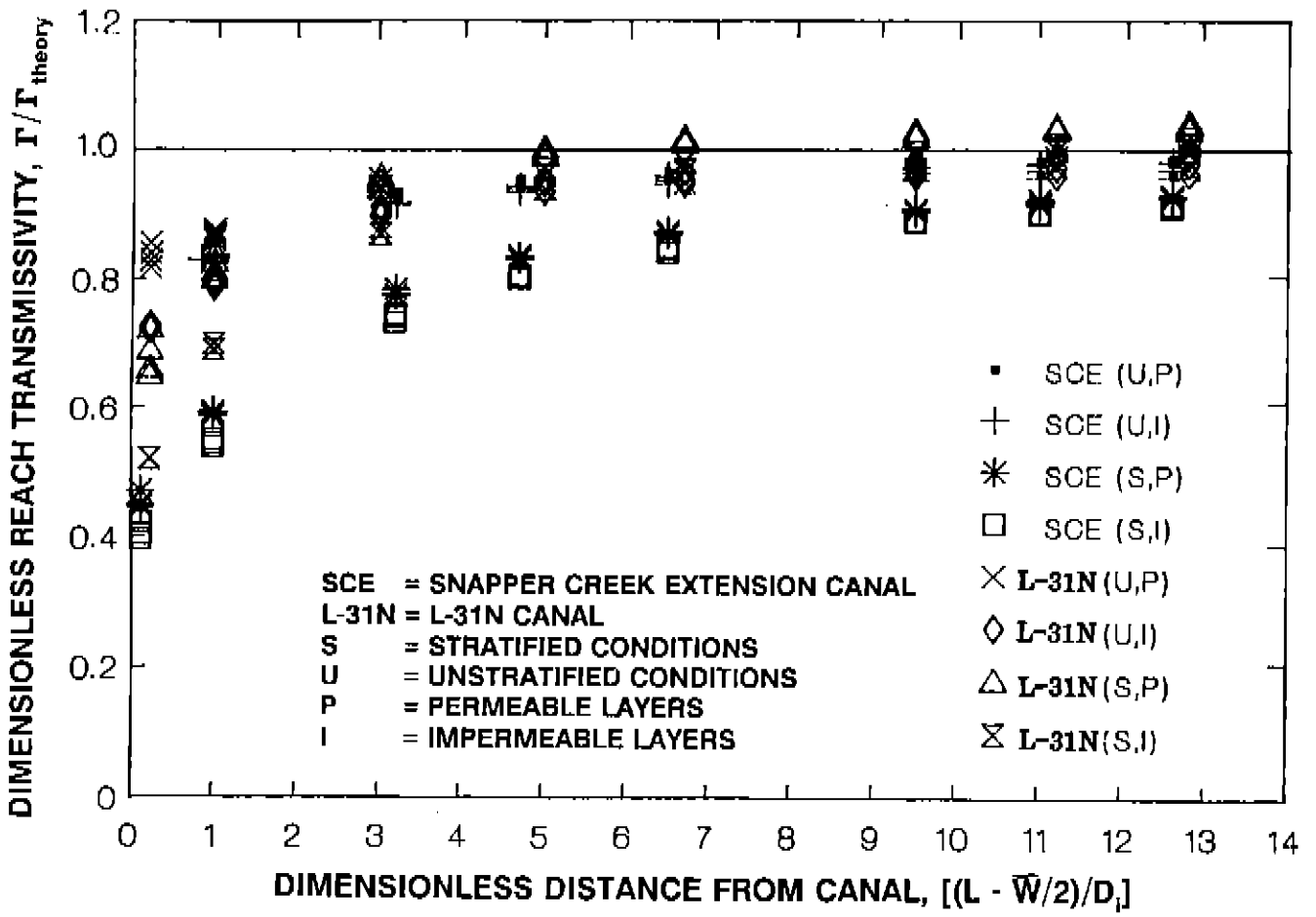

Figure 11. Relation between dimensionless reach transmissivity and dimensionless distance from canal.

In addition to models that use cell-averaged heads at each node point, a separate class of models exists in which the nodal heads are taken as the actual heads at the nodes. In such models, it is appropriate to specify the nodal reach transmissivity to be equal to the local reach transmissivity (Γ_L). However, the modeler needs to recognize the singularity that exists when the channel is completely open to the aquifer ($\Gamma_L = \infty$). If this case occurs in natural channels, which is seldom, leakage out of the channel must be related to drawdowns at nodes some distance away from the channel.

FIELD TESTS OF THE METHOD

The functional form of the reach transmissivity for asymmetrical drawdowns around channels underlain by a semipermeable layer of bed material was presented and verified by comparing the proposed analytical formulation with the simulations of a fine-scale numerical model. Natural channels can deviate significantly from the idealized conditions described by the theoretical formulation. For example, hydraulic connection between the channel and the aquifer can be highly variable around the channel perimeter, or the drawdowns can be nonuniform along the channel. To validate the proposed formulation in natural channels, a field study was conducted at L-31N Canal and Snapper Creek Extension Canal.

Design of Experiments

The objective of the field study was to determine if leakages predicted by the theory at L-31N Canal and Snapper Creek Extension Canal agree with field measurements. The procedure involved the installation of AVM systems (Laenen, 1985; Laenen and Curtis, 1989) at 1-mile intervals along the channels to measure discharges, stages recorders at each section to measure the canal stages, and monitoring wells to measure the heads adjacent to the channels. The canal stage and water-table altitudes were then subtracted to obtain the drawdowns adjacent to the canals. Leakages between AVM stations were determined by subtracting the measured upstream and downstream discharges. The measured relation between the drawdown and leakage (the reach transmissivity function) was then compared with the theoretical relation given by equation 15. Experiments were conducted for 6 weeks, with at least 24 hours elapsing between each experiment. The field measurements obtained during this study are given in appendixes I to IV. To ensure the integrity of these measurements, the criteria required that no rainfall occurred within the 24 hours preceding each experiment and that wind effects were negligible.

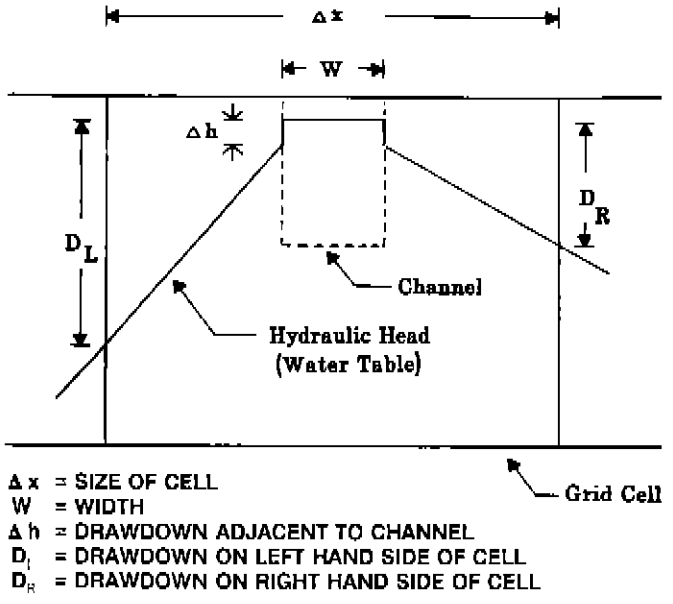

Figure 12. Intracell-head distribution in numerical model.

L-31N Canal

The site layout of L-31N Canal is shown in figure 13. At this site, there are three AVM stations at 1-mile intervals. At each AVM station, transducers were mounted on vertical poles within the channel. In accordance with guidelines established by Laenen and Smith (1983), a crossed acoustic path was used to minimize errors associated with variations in streamflow direction.

A typical AVM station is shown in figure 14. A major problem in using an AVM system to measure leakage is that the AVM measures only the discharge between transducer mounts and not the flow between the sides of the channel and the transducers. This outside flow is on the same order of magnitude as the leakage and, therefore, needs to be estimated. To alleviate the problem, a Neil-Brown current meter was used to measure total discharge across each AVM section, and hence, determine the percentage of total flow between the transducers. These results, given in table 1, indicate that the percentage of total flow outside the transducers remains relatively constant. Also, because the flows measured in this study (appendixes I and II) did not deviate significantly from those shown in table 1, the average percentages shown in the table were used to correct the measured flow between transducers and, thus, obtain total flow across the entire channel.

Stage recorders installed at each AVM section measured canal stages at 15-minute intervals. Clusters of monitoring wells were placed along three transects passing through the AVM stations (fig. 13). The depth and location of the monitoring wells are given in table 2. Each well cluster typically had wells screened at the top and bottom of the aquifer with a few wells screened in the middle. Screen lengths of 2 feet were used at the monitoring well locations. Transects at miles 1 and 3 measured drawdowns in the immediate vicinity of the channel, whereas the transect at mile 2 measured the drawdowns up to 550 feet (14 aquifer depths) away from the channel. The drawdowns measured at these outside wells were primarily used in validating the proposed theory.

Snapper Creek Extension Canal

The site layout of Snapper Creek Extension Canal is shown in figure 15. The field instrumentation is deployed somewhat differently from that at L-31N Canal because the monitoring well clusters were in place before the inception of the study. A notable feature of Snapper Creek Extension Canal is a side channel aligned with the monitoring well transect. This side channel probably has a significant effect on the uniformity of the drawdowns adjacent to the main channel—a factor considered during the analysis of the measurements.

The monitoring well locations are given in table 2. At each cluster, wells were screened at the top and bottom of the aquifer as well as within the semi-impermeable lower boundary of the aquifer. Screen lengths of 2 feet were used at the monitoring well locations. The AVM stations are 0.5 mile north and south of the monitoring well transect, and the stations are identical to those used at L-31N Canal (fig. 14).

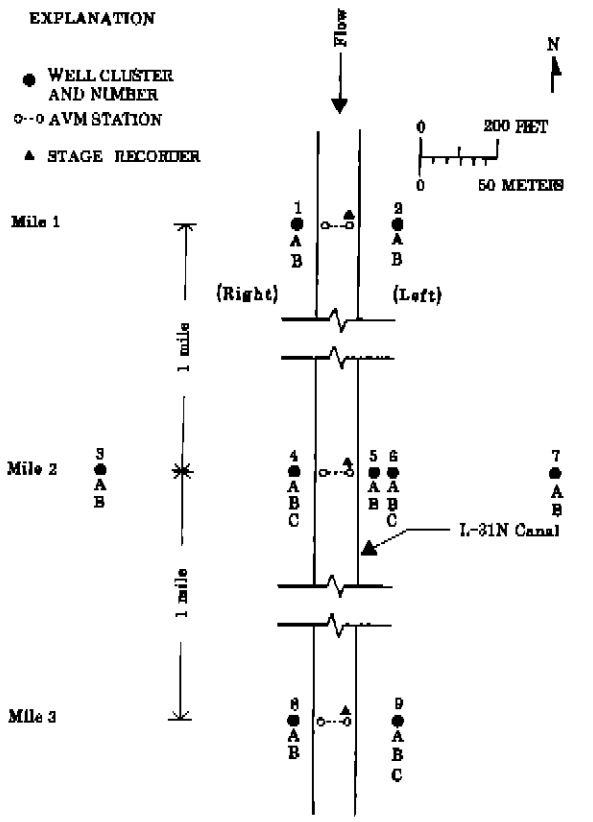

Figure 13. Field instrumentation at L-31N Canal.

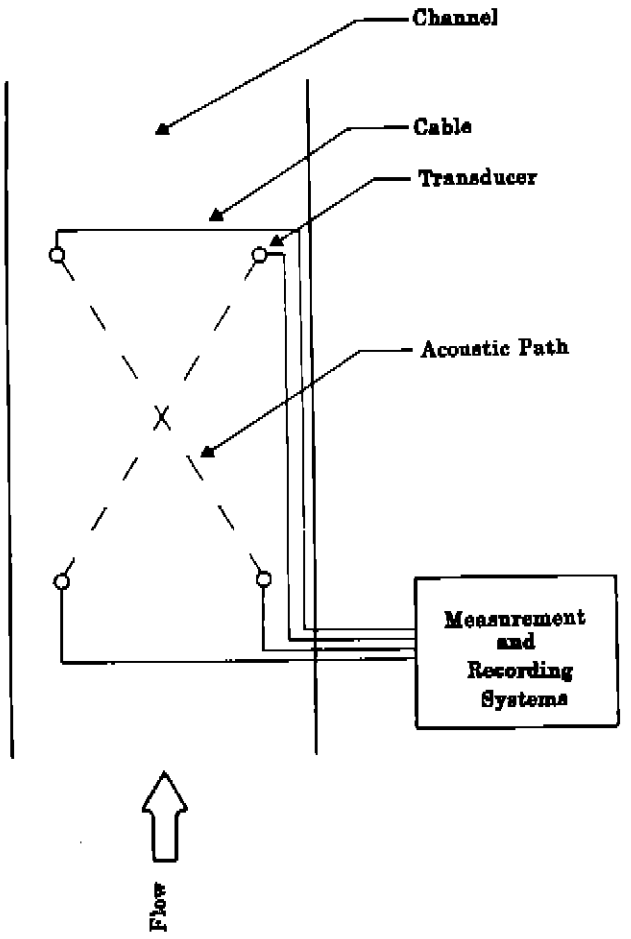

Figure 14. Typical acoustic velocity meter station.

Confidence Limits

An important aspect of data analysis is knowing the accuracy of measured data. This information is necessary in establishing confidence limits as well as determining the validity of any hypotheses.

Head measurements were made using chalked steel tape, generally accurate within 0.005 feet; therefore, the accuracy of the measured drawdowns (difference of head measurements) may be taken as ±0.01 foot. The accuracy of velocity measured by the AVM was studied by Laenen and Curtis (1989). They give the velocity errors for different path lengths and transducer frequencies for "one interrogation per measurement," on the basis of an assumed signal-detection error of one-quarter cycle of the transducer frequency. In the present study, 200-kHz transducers were used, and the path length ranged from 93 to 135 feet at Snapper Creek Extension Canal and L-31N Canal, respectively). For 200-kHz transducers and a path length of 164 feet, Laenen and Curtis (1989) give a one-interrogation velocity error of ±0.124 ft/s. Inasmuch as this error corresponds to a path length that is longer than that used for this study, and because accuracy increases with path length, ±0.124 ft/s can be considered a conservative estimate of the one-interrogation velocity error. According to Laenen and Curtis (1989), if n interrogations are used to estimate the velocity, then the error in the measured velocity ($\bar{v}_{err}$) is given by

$$\bar{v}_{err} = \frac{v_{err}}{\sqrt{n}} , \qquad (28)$$

where v_{err} is one-interrogation velocity error.

In this study, 20 interrogations for each measurement were made (4 minute^{-1} for 5 minutes). Substituting n = 20 and v_{err} = ±0.124 ft/s into equation 28 yields a velocity error ($\bar{v}_{err}$) of ±0.0277 ft/s. AVM systems measure average velocity along the acoustic path, and it is generally assumed that the cross-sectional averaged velocity ($\bar{v}$) is related to the path averaged velocity ($\bar{v}_p$) according to the expression (Laenen, 1985),

$$\bar{v} = \frac{K \bar{v}_p}{\cos \theta} , \qquad (29)$$

where θ is the angle that the acoustic path makes with the flow direction, and K is a constant, generally called the "K coefficient," which depends on the velocity distribution in the channel.

Laenen (1985) presented an analytical expression for evaluating K, assuming that the one-dimensional Prandtl-von Karman velocity distribution is applicable. However, in cases where the channel is relatively narrow, the sides of the channel may induce a significant two-dimensional velocity distribution. In such cases, theoretical velocity distributions given by Chiu and others (1976) and Chiu (1988) may be more appropriate. In this study, preliminary analyses indicated that the one-dimensional and two-dimensional distributions yielded almost identical K coefficients at

Table 1. Percentage of total flow between transducers at L-31N Canal

[Total flow in cubic feet per second. Asterisk (*) denotes average]

Mile	Date of measurement	Total flow	Percentage of flow between transducers
1	3-23-89	696	93.5
	3-27-89	737	93.7
	4-3-89	639	94.3
			93.8*
2	3-23-89	629	94.9
	3-27-89	669	95.2
	4-3-89	685	92.5
			94.2*
3	3-23-89	560	96.8
	3-27-89	596	96.0
	3-29-89	629	94.2
	4-3-89	577	94.8
			95.5*

Table 2. Monitoring well locations at L-31N Canal and Snapper Creek Extension Canal
[Bottom 2 feet of each well is screened]

Well number	L-31N		Snapper Creek Extension	
	Distance from edge of canal (feet)	Bottom altitude of well (feet, above sea level)	Distance from edge of canal (feet)	Bottom altitude of well (feet, above sea level)
1A	40	0.0	535	-15.0
1B	40	-47.1	535	-44.7
1C			535	-125.0
2A	93	.2	135	-14.2
2B	93	-52.0	135	-44.2
2C			135	-94.4
3A	550	-1.4	35	-17.8
3B	550	-47.7	35	-54.9
3C			35	-101.3
4A	45	- .8	20	-16.1
4B	45	-18.1	20	-64.1
4C	45	-53.7	20	-114.0
5A	44	- .2	70	-12.3
5B	44	-55.9	70	-41.3
5C			70	-94.2
6A	81	- .9	270	-14.6
6B	81	-19.4	270	-45.1
6C	81	-54.8	270	-95.0
7A	500	-2.5	520	-15.6
7B	500	-46.1	520	-45.8
7C			520	-95.6
8A	40	.2		
8B	40	-45.6		
9A	110	.6		
9B	100	-43.7		
9C	100	-160.0		

L-31N Canal, whereas at Snapper Creek Extension Canal, K coefficient estimates using a two-dimensional velocity distribution typically were about 10 percent less than those obtained using the one-dimensional distribution. These results are consistent in that L-31N Canal is a very wide channel with a width-to-depth ratio of 6.3, whereas Snapper Creek Extension Canal is narrower with a ratio of 2.9. If K coefficients are estimated at L-31N Canal using a one-dimensional Prandtl-von Karman velocity distribution, and at Snapper Creek Extension Canal using a two-dimensional velocity distribution (Chiu and others, 1976), then the error in the discharge measurement can be estimated by

$$\text{Discharge error} = \pm \left[\frac{K \bar{v}_{err}}{\cos \theta} A_o + A_{err} \bar{v} \right], \quad (30)$$

where A_o is the flow area, and A_{err} is the error in estimating A_o. Leakages are obtained by subtracting upstream and downstream discharge, and thus, the leakage confidence limits are given by

$$\text{Leakage error} = \pm \left[\bar{v}_{err} \left(\frac{K_u A_u}{\cos \theta_u} + \frac{K_d A_d}{\cos \theta_d} \right) + A_{err} (\bar{v}_u + \bar{v}_d) \right], \quad (31)$$

where subscripts u and d refer to upstream and downstream measurements, respectively, and it is assumed that errors in estimating the AVM path velocity and flow area are the same at the upstream and downstream sections.

The reach transmissivity is defined as the leakage divided by drawdown; therefore, the percentage error in the reach transmissivity is approximately equal to the sum of the

percentage error in the leakage and drawdown. Noting that the leakage error is given by equation 31, the confidence limits in the reach transmissivity (Γ_R) are given by

$$\text{Reach transmissivity error} = \pm \left[\frac{A_u\bar{v}_u - A_d\bar{v}_d}{D_R} \cdot \frac{D_{err}}{D_r} + \frac{\left[\bar{v}_{err}\left(\frac{K_uA_u}{\cos\theta_u} + \frac{K_dA_d}{\cos\theta_d}\right) + A_{err}(\bar{v}_u + \bar{v}_d)\right]}{D_R} \right], \quad (32)$$

where D_R is drawdown to the right side of the channel, and D_{err} is the error in estimating D_R.

The confidence limits developed here are measures of the extent to which the field measurements may be expected to vary from the theoretical expressions, provided the theoretical expressions are correct. Therefore, if the field measurements are within the confidence limits of the theory, the theory is considered valid.

Analysis of Results

The theoretical reach transmissivity (Γ_R) is given by equation 15, which expresses the reach transmissivity (Γ_R) in terms of a formation parameter (Γ_o), local reach transmissivity (Γ_L), and drawdown (D_L and D_R). Also, Γ_o, D_L, and D_R depend on the distance at which these quantities are measured. The theoretical formulation provides excellent agreement with a fine-scale numerical leakage model when Γ_o, D_L, and D_R are evaluated greater than 10 aquifer depths from the channel. The leakage characteristics of natural channels may differ significantly from the idealized conditions described by equation 15. The significance of this deviation at L-31N and Snapper Creek Extension Canals is discussed in the following sections.

L-31N Canal

At L-31N Canal, AVM stations are at miles 1, 2, and 3. Drawdowns around mile 2 are measured up to 550 feet (14 aquifer depths) from the side of the channel (fig. 13). With this arrangement, the reach transmissivity can be estimated for the reaches upstream and downstream of mile 2 as well as the overall reach transmissivity between miles 1 and 3. In determining the reach transmissivities for miles 1 to 2 and 2 to 3, on the basis of drawdowns measured at mile 2, it is necessary to assume that the drawdowns around the channel remain relatively uniform along the channel. The validity of this assumption was evaluated by comparing synoptic measurements of the average drawdown at monitoring wells 1A and 2A (mile 1), 4A and 6A (mile 2), and 8A and 9A (mile 3). These well pairs are approximately the same distance from the channel and are completed at about the same altitude in the upper part of the aquifer. The relation between the average drawdowns at miles 1, 2, and 3 is shown in figure 16.

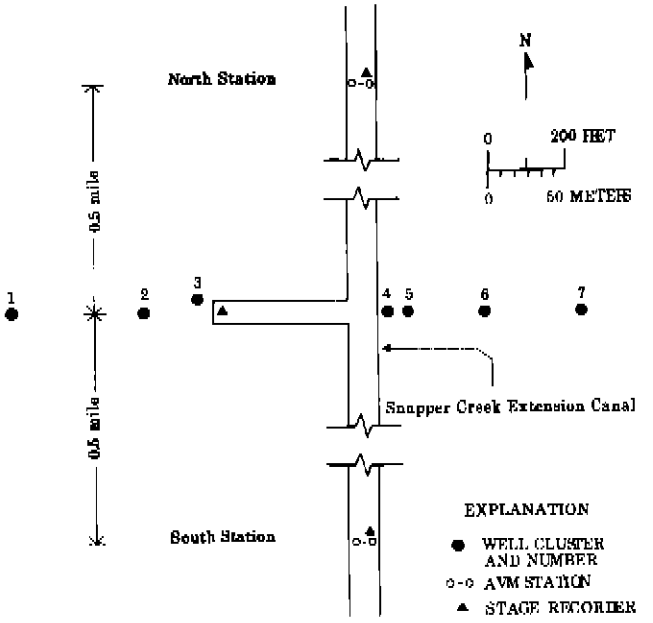

Figure 15. Field instrumentation at Snapper Creek Extension Canal.

If all drawdowns were identical, then all points would lie on the uniform drawdown line, which has a slope of 1. Most measurements lie close to the uniform drawdown line, indicating that assuming approximate uniformity in drawdown along the channel was reasonable.

This study defines the left and right sides of the channel looking downstream. Logistical problems prevented the outside well clusters at mile 2 from being exactly equidistant from the sides of the channel. The outside clusters on the left and right sides are 500 feet and 550 feet, respectively, from the sides of the channel. To obtain drawdown estimates in areas 500 feet from each side of the channel, the drawdown at 500 feet from the right side was interpolated from measurements at well clusters 3 and 4 (fig. 13). However, because the interpolated point was near the measurement location, the estimation errors were probably small. Combining the mile 2 drawdowns at 500 feet (13 aquifer depths) from the channel with measured leakages between miles 1 and 3, the relation can be determined between the reach transmissivity (Γ_R) and the drawdown ratio (D_L/D_R). These measurements are compared with theory in figure 17.

To assess the significance of the deviations of the measurements from theory, the confidence limits derived from measurement errors need to be established. The confidence limits associated with each measurement point are given by equation 32, and the range of confidence limit parameters observed during this study are given in table 3. The minimum confidence limits associated with the entire set of measurement points were determined, and the deviation between the measurements and theory relative to these confidence limits was compared. The comparison provides the most stringent test of the proposed theory for the range of conditions experienced during this study.

According to equation 32, the minimum confidence limits are obtained by using the minimum values given in table 3. For this reason, the maximum drawdown (D_R) was employed. Selecting the appropriate extreme values (table 3), the minimum confidence limits for reach transmissivity are ±410 (ft^3/s)/mi/ft. These confidence limits for reach transmissivity are compared with the deviation of the measurements from theory in figure 17. Considering inherent measurement errors, the data show excellent agreement with theory and seem to validate the proposed formulation. The reach transmissivity function has a slope of 130 (ft^3/s)/mi/ft and intersects the D_L/D_R axis at -1 (as predicted by theory). To assess the uniformity of the reach transmissivity function, leakages from miles 1 to 2 and 2 to 3 were considered separately (fig. 18). The reach transmissivity function is approximately uniform over each of these reaches, although somewhat more scatter is observed between miles 2 and 3.

The reach transmissivity function in figures 17 and 18 only applies for drawdowns measured 500 feet from the side of the channel. The basic leakage relation developed earlier (eqs. 8 and 15) gives the reach transmissivity at any distance from the channel in terms of the local reach transmissivity (Γ_L) and the transmissivity of the formation (T). Because the slope of the reach transmissivity function generally is given by $\Gamma_L\Gamma_o/2(\Gamma_L + \Gamma_o)$ (eq. 15), where Γ_o depends only on T and the distance from the side of the channel, L - W/2 (eq. 8), then Γ_L and T can be conveniently determined by obtaining the reach transmissivity function at two distances from the channel. By equating the slopes of these functions to $\Gamma_L\Gamma_o/2(\Gamma_L + \Gamma_o)$, one may solve for Γ_L and T (from Γ_o), and thus describe the reach transmissivity function for drawdowns measured at any distance from the channel.

The reach transmissivity function between miles 1 and 3, on the basis of drawdowns measured 40 feet from the channel at mile 2, is shown in figure 19. The measurements agree with the proposed theory within the confidence limits imposed by measurement errors. Again, the minimum confidence limits associated with conditions encountered during this study (table 3), ±410 (ft^3/s)/mi/ft, are used. Leakages between miles 1 and 2 and miles 2 and 3 were considered separately and compared with the average reach transmissivity in figure 20. These results indicate leakage characteristics are approximately uniform along the channel. Moreover, the verification study presented earlier showed that the theoretical

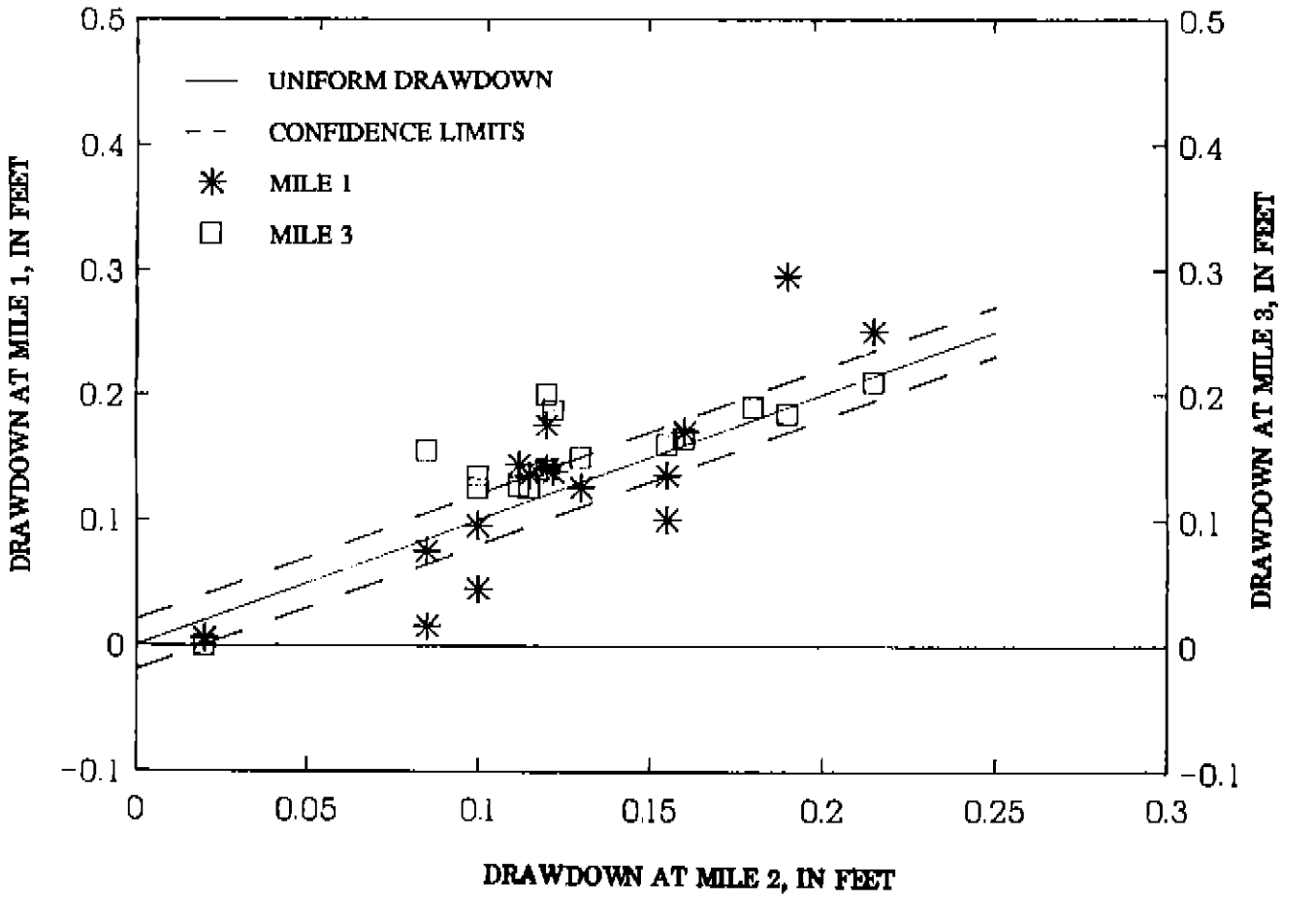

Figure 16. Relation between drawdown at mile 2 and drawdown at miles 1 and 3 of L-31N Canal.

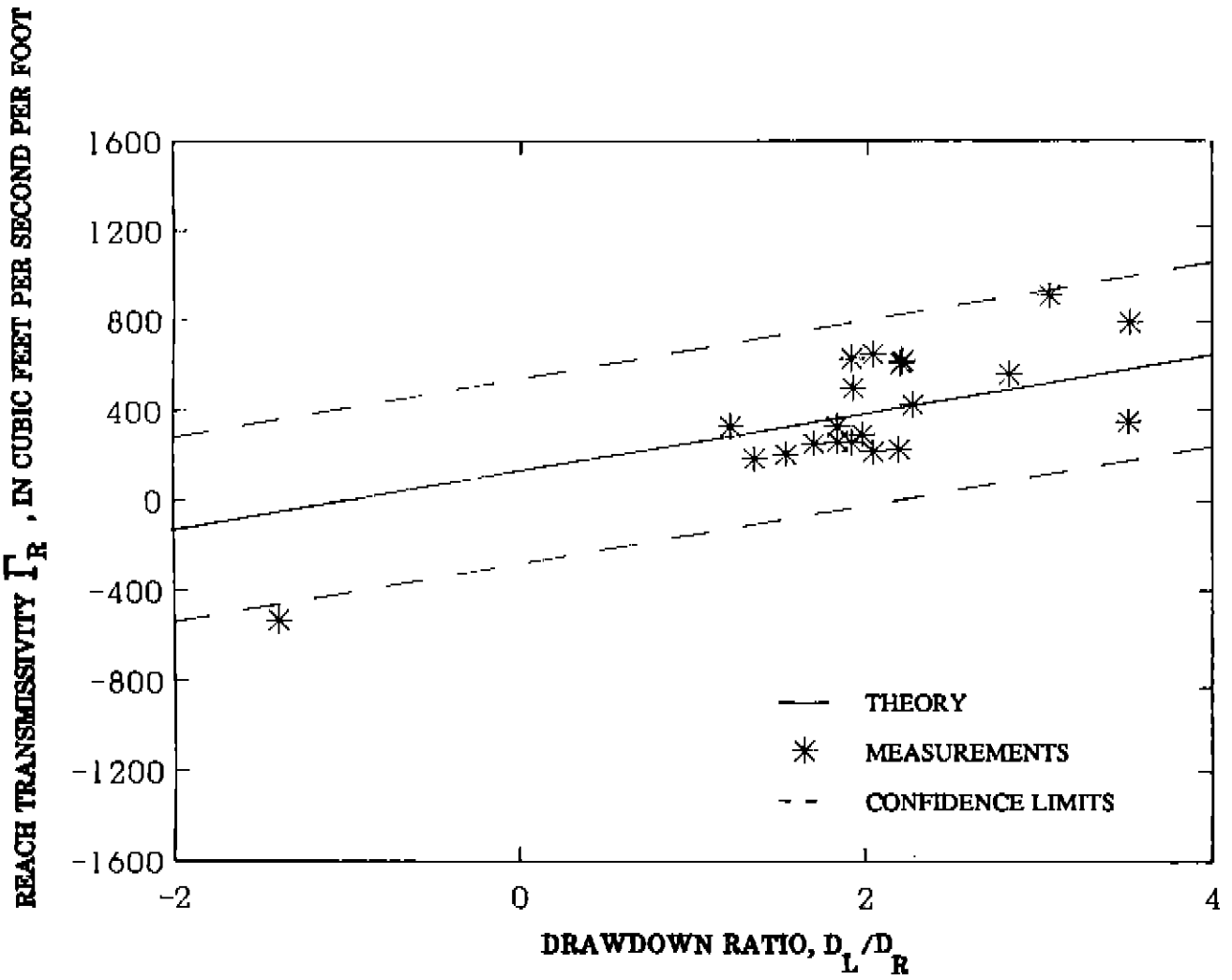

Figure 17. Average reach transmissivity between miles 1 and 3, 500 feet from L-31N Canal.

reach transmissivity function overpredicts the actual reach transmissivity in areas near the channel (fig. 11). In the present case, at 40 feet (one aquifer depth) from the channel, the reach transmissivity is expected to be about 80 percent of the theoretical value. Accordingly, the slope of the measured reach transmissivity function, 225 $(ft^3/s)/mi/ft$, can be equated to $0.8\ \Gamma_L\Gamma_o/2(\Gamma_L + \Gamma_o)$ and the drawdown ratio intercept to -0.8.

Based on the slope of the reach transmissivity at 500 and 40 feet, the basic leakage parameters are Γ_L = 630 $(ft^3/s)/mi/ft$ and T = 1.8×10^6 ft^2/d, where T is obtained from Γ_o according to equation 8. Although there are no independent studies from which to compare Γ_L, T was determined to be 1.7×10^6 ft^2/d by Fish and Stewart (1990) using pump tests. This value closely agrees with that determined in this study (within 6 percent) and reflects the validity of the analytical procedures used. Reliable determination of transmissivity in this particular aquifer is very difficult to obtain with pump tests because of the enormous rate at which water must be pumped to produce measurable drawdowns. Using the natural leakage out of the channel as a source of water, and measuring the drawdowns at two symmetric areas about the channel, solves both the pump-capacity problem and the water-disposal problem associated with pump tests.

At L-31N Canal, the proposed reach transmissivity formulation is valid and correctly predicts the functional relation between the reach transmissivity and the drawdown ratio. Furthermore, field measurements, when analyzed using the proposed theoretical relation, yield the fundamental leakage parameters. One of these parameters is the formation transmissivity, which closely agreed with previous estimates on the basis of pump tests.

Snapper Creek Extension Canal

At Snapper Creek Extension Canal, measurements using the AVM system were unable to adequately resolve the mean velocity in the channel because the measured velocities were less than the sampling error of the AVM (±0.0277 ft/s) in all but one experiment (appendix III). The mean velocities measured at the north and south AVM stations were 0.015 and 0.016 ft/s, respectively.

Table 3. Parameter values and associated errors of estimate at L-31N Canal

[Leakage, in cubic feet per second per mile; drawdown, in feet; velocity, in feet per second; area, in square feet. Area error, encompases 2 percent of total area]

Parameters	Expression	Range	Average
Leakage	$A_u\bar{v}_u - A_d\bar{v}_d$	4 - 112	44
Drawdown			
at 500 feet	D	0.05 - 0.23	.11
at 40 feet	D	0.00 - 0.21	.11
Drawdown error	D_{err}	0.01	.01
Flow velocity	$\bar{v}_u + \bar{v}_d$	0.783 - 1.305	1.090
Velocity error	$\bar{v}_{err}$	0.0277	.0277
Adjusted flow area	$K_uA_u/\cos\theta_u + K_dA_d/\cos 0_d$	2,787 -3 ,245	3,104
Area error	A_{err}	22 - 28	25

Despite the inability to measure leakage directly, leakage can be indirectly estimated. At this site, flow to the west can be estimated by multiplying the head gradient between well clusters 1 and 2 by the transmissivity of the formation, assumed to be 1×10^6 ft^2/d (Fish and Stewart, 1990). Similarly, the flow to the east can be estimated by multiplying the head gradient between well clusters 6 and 7 by the transmissivity. By adding the westerly and easterly flows, an estimate of the channel leakage can be obtained.

For each of the field experiments, the estimated reach transmissivity was plotted against the drawdown ratio between well clusters 1 (= D_L) and 7 (= D_R). The proposed linear formulation provides a good approximation to the results (fig. 21). Furthermore, this linear relation is insensitive to the assumed transmissivity because a different aquifer transmissivity would adjust the estimated reach transmissivity by a constant factor. Hence, a linear approximation would still be appropriate, but with an adjusted slope.

All measured drawdown ratios were negative, reflecting the condition that the drawdown was always above the canal stage on the east ($D_R < 0$) and below the canal stage on the west ($D_L > 0$). At the monitoring well transect, the outer wells are about 530 feet from the sides of the channel, and with an aquifer transmissivity of 1×10^6 ft^2/d, Γ_o = 230 (ft^3/s)/mi/ft (eq. 8) is obtained. Combining this value with the slope of the reach transmissivity function [= $\Gamma_o\Gamma_L/2(\Gamma_o + \Gamma_L)$], 72 (ft^3/s)/mi/ft, the value Γ_L = 385 (ft^3/s)/mi/ft is obtained. More accurate measurements of discharge and more detailed measurements of drawdown are necessary to obtain reliable estimates of the local and formation reach transmissivities.

At Snapper Creek Extension Canal, the reach transmissivity analysis is approximate and only applicable at the monitoring well transect. At this section, it was necessary to include the length of the side channel in the width of the stream (fig. 15), and the drawdown and reach transmissivities show the same functional relation predicted by theory.

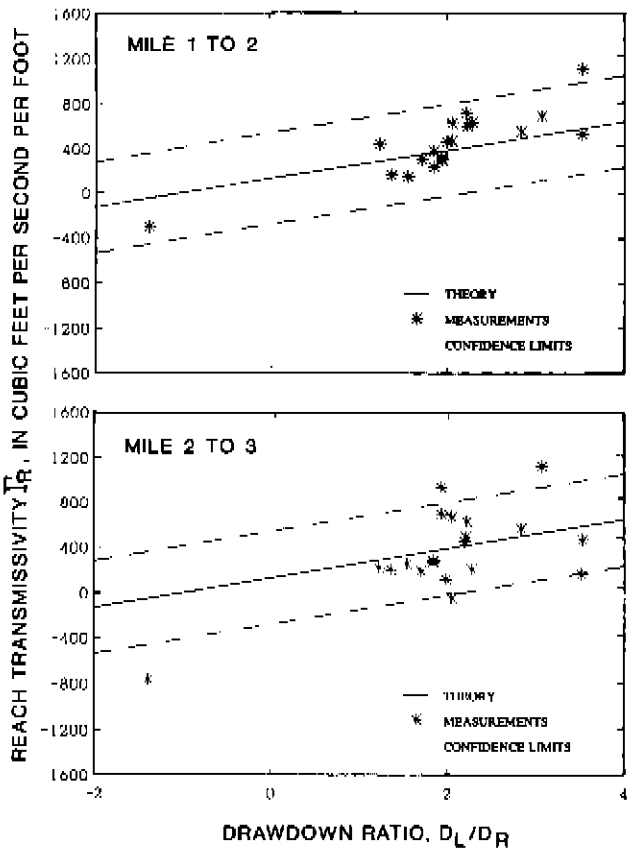

Figure 18. Reach transmissivities for miles 1 to 2 and 2 to 3, 500 feet from L-31N Canal.

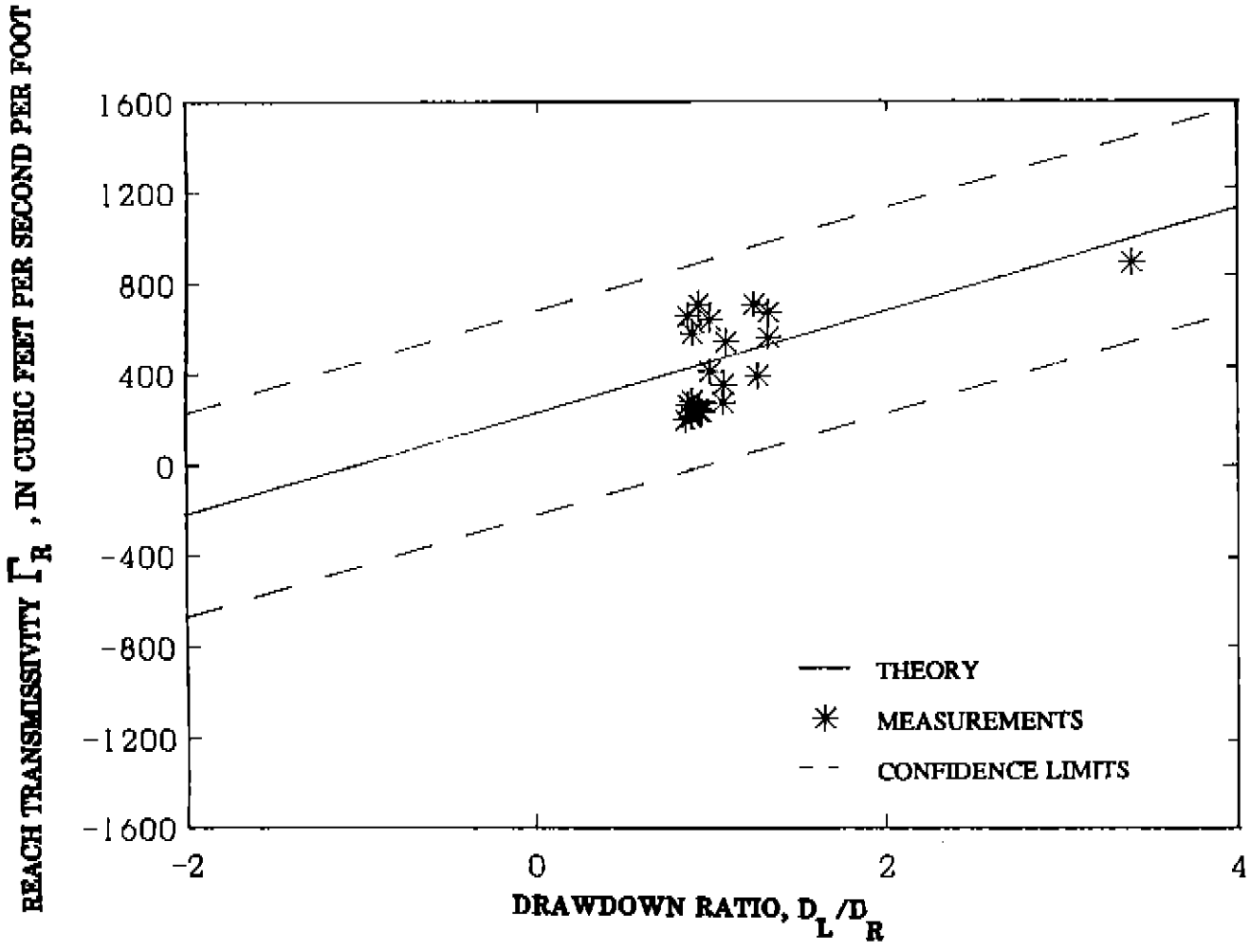

Figure 19. Average reach transmissivity between miles 1 and 3, 40 feet from L-31N Canal.

SUMMARY AND CONCLUSIONS

This study has described a method to quantify leakage out of channels that partially penetrate the Biscayne aquifer and are underlain by semipermeable bed materials. The leakage characteristics of the channels are described in terms of a reach transmissivity equal to the volume flow rate out of the channel per unit channel length divided by the drawdown measured at a particular distance from one side of the channel. A theoretical formulation relates the reach transmissivity of the channel to the ratio of drawdowns on both sides of the channel, the transmissivity of the formations, the mean width of the channel, the distance of the drawdown measurement from the center of the channel, and the local transmissivity of the semipermeable layer lining the channel.

The proposed formulation was verified at two canals, L-31N Canal and Snapper Creek Extension Canal, with distinctly different channel shapes in Dade County, Fla. The theoretical results were compared with results obtained from a fine-scale numerical model, which can accurately simulate the leakage process. Comparisons between theoretical and numerical results showed excellent agreement. Specifically, if the drawdowns were measured at about 13 aquifer depths from the side of the channel, the reach transmissivity was insensitive to the hydraulic conductivity distribution and depended only on the formation transmissivity. Furthermore, leakage characteristics of a channel open to the aquifer did not change significantly when an impermeable layer covered the channel bottom; primarily, because most leakage is out of the sides.

The decrease in overall reach transmissivity as the local reach transmissivity decreases was accurately described by the theoretical formulation. Because the proposed formulation implicitly depended on the validity of the Dupuit-Forcheimer assumption, the accuracy of the theory decreases as drawdowns are measured closer to the channel. This limitation was investigated by comparing numerical and theoretical results for various measurement distances. Beyond 10 aquifer depths from the side of the channel, theoretical and numerical results differed by less than 10 percent.

Reach transmissivities used in regional numerical ground-water models are commonly based on the average drawdown in a cell. An analysis of the relation between the cell reach transmissivity and the theoretical formulation developed in this study showed how the results of this study could be employed in numerical models. Also, it was shown that the reach transmissivity in numerical models was inversely proportional to the cell size.

The proposed reach transmissivity formulation was validated in the field by comparing the measured reach transmissivity functions with those predicted by theory. Both L-31N Canal and Snapper Creek Extension Canal showed good agreement with the theoretical reach transmissivity function. At L-31N Canal, the local reach transmissivity and formation transmissivity were obtained by combining theory and measurements. These derived leakage parameters are fundamental in accurately describing the volume flux between the channel and aquifer under any drawdown scenario.

SELECTED REFERENCES

Bouwer, Herman, 1965, Theoretical aspects of seepage from open channels: American Society of Civil Engineers Journal of the Hydraulics Division, v. 91, no. HY3, p. 37-59.

——— 1969, Theory of seepage from open channels: Advances in Hydroscience, v. 5, p. 121-172.

——— 1978, Groundwater hydrology: New York, McGraw-Hill Book Company, 480 p.

Chiu, C.L., 1988, Entropy and 2-D velocity distribution in open channels: American Society of Civil Engineers Journal of the Hydraulics Division, v. 114, no. 7, p. 738-756.

Chiu, C.L., Lin, H.C., and Mizumura, K., 1976, Simulation of hydraulic processes in open channels: American Society of Civil Engineers Journal of the Hydraulics Division, v. 102, no. HY2, p. 185-205.

Collins-George, N., and Smiles, D.E., 1963, A study of some aspects of the hydrology of some irrigated soils of western New South Wales: Australian Journal of Soil Research, v. 1, p. 17-27.

Dachler, R., 1936, Grundwasserstromung: Springer, Vienna.

Dillon, P.J., and Liggett, J.A., 1983, An ephemeral stream-aquifer interaction model: Water Resources Research, v. 19, no. 3, p. 621-626.

Ernst, L.F., 1962, Grondwaterstromingen in de verzadigde zone en hun berekening bij de aawezighei van horizontale evenwijdige open leidingen: Verslag. Landbouwk. Onderzock, v. 67.15.

Fish, J.E., and Stewart, Mark, 1990, Hydrogeology of the surficial aquifer system, Dade County, Florida: U.S. Geological Survey Water-Resources Investigations Report 90-4108.

Flug, M., Abi-Ghanem, G.V., and Duckstein, L., 1980, An event based model of recharge from an ephemeral stream: Water Resources Research, v. 16, no. 4, p. 685-690.

French, R.H., 1985, Open-channel hydraulics: New York, McGraw-Hill Book Company, 705 p.

Hantush, M.M., and Mariño, M.A., 1989, Chance-constrained model for management of stream-aquifer system: Journal of Water Resources Planning and Management, v. 115, no. 3, p. 259-277.

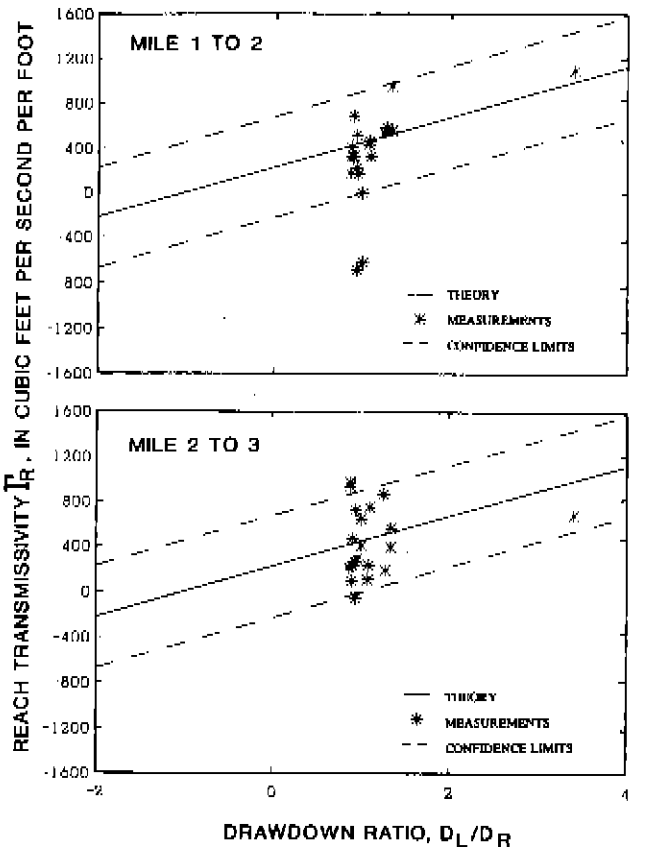

Figure 20. Reach transmissivities for miles 1 to 2 and 2 to 3, 40 feet from L-31N Canal.

Harr, M.E., 1962, Groundwater and seepage: New York, McGraw-Hill Book Company, 315 p.

Herbert, Robin, 1970, Modelling partially penetrating rivers on aquifer models: Ground Water, v. 8, p. 29-36.

Jenkins, C.T., 1968, Techniques for computing rate and volume of stream depletion by wells: Ground Water, v. 6, p. 37-46.

Jorgensen, D.G., Signor, D.C., and Imes, J.L., 1989, Accounting for intracell flow in models with emphasis on water table recharge and stream-aquifer interaction: (1) problems and concepts; and (2) a procedure: Water Resources Research, v. 25, no. 4, p. 669-684.

Klein, Howard, and Hull, J.E., 1978, Biscayne aquifer, southeast Florida: U.S. Geological Survey Water-Resources Investigations Report 78-107, 57 p.

Klein, Howard, and Sherwood, C.B., 1961, Hydrologic conditions in the vicinity of levee 30, north Dade County, Florida: Florida Geological Survey Report of Investigations 24, part I, 24 p.

Labowski, J.L., 1988, Geology, hydrology, and water monitoring program, northwest wellfield protection area: Dade County Department of Environmental Resources Management Technical Report No. 88-3, 32 p.

Laenen, Antonius, 1985, Acoustic velocity meter systems: U.S. Geological Survey Techniques of Water-Resources Investigations, book 3, chap. A17, 38 p.

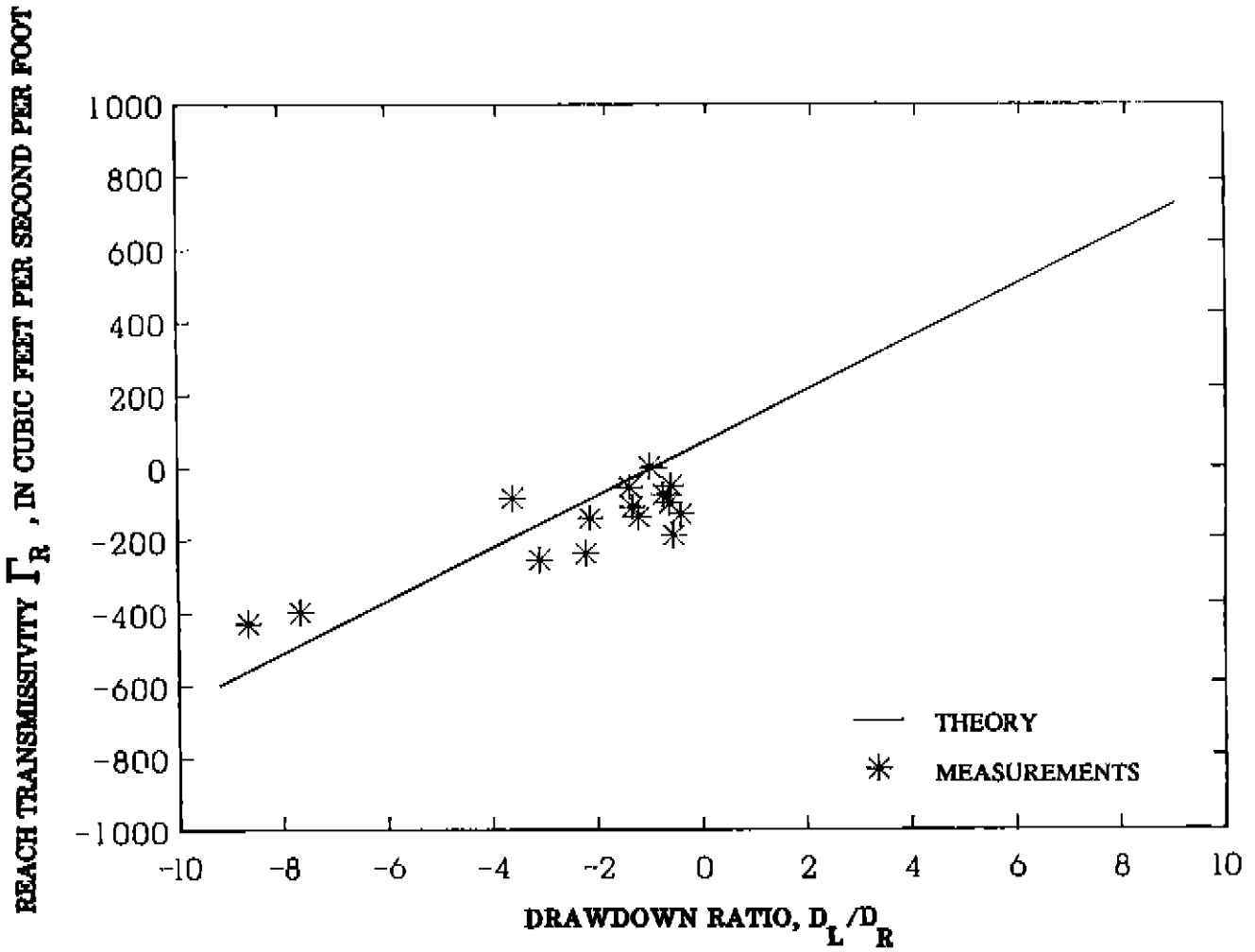

Figure 21. Reach transmissivity at Snapper Creek Extension Canal.

Laenen, Antonius, and Curtis, R.E., 1989, Accuracy of acoustic velocity metering systems for measurement of low velocity in open channels: U.S. Geological Survey Water-Resources Investigations Report 89-4090, 15 p.

Laenen, Antonius, and Smith, Winchell, 1983, Acoustic systems for the measurement of streamflow: U.S. Geological Survey Water-Supply Paper 2213, 26 p.

Leach, S.D., Klein, Howard, and Hampton, E.R., 1972, Hydrologic effects of water control and management of southeastern Florida: Florida Bureau of Geology Report of Investigations 60, 115 p.

MacVicar, T.K., VanLent, Thomas, and Castro, Alvin, 1984, South Florida water management model, documentation report: South Florida Water Management District Technical Publication 84-3, 123 p.

McDonald, M.G., and Harbaugh, A.W., 1988, A modular three-dimensional finite-difference ground-water flow model: U.S. Geological Survey Techniques of Water-Resources Investigations, book 6, chap. A1.

Meyer, F.W., 1971, Seepage beneath Hoover Dike southern shore of Lake Okeechobee, Florida: Florida Bureau of Geology Report of Investigations 58, 98 p.

Miller, W.L, 1978, Effects of bottom sediments on infiltration from the Miami and tributary canals to the Biscayne aquifer, Dade County, Florida: U.S. Geological Survey Water-Resources Investigations Report 78-36, 69 p.

Mishra, G.C., and Seth, S.M., 1988, Seepage from a river of large width to a shallow water table aquifer: Ground Water, v. 26, no. 4, p. 439-444.

Morel-Seytoux, H.J., 1964, Domain variations in channel seepage flow: American Society of Civil Engineers Journal of Hydraulics Division, v. 90, no. HY2, p. 55-79.

——— 1975, A combined model of water table and river stage evolution: Water Resources Research, v. 11, no. 6, p. 968-972.

Morel-Seytoux, H.J., and Daly, C.J., 1975, A discrete kernel generator for stream-aquifer studies: Water Resources Research, v. 11, no. 2, p. 253-260.

Morel-Seytoux, H.J., Illangasekare, T., and Peter, G., 1979, Field verification of the concept of reach transmissivity: Proceedings of the IAHS-AISH Canberra Symposium, Publication No. 128, p. 355-359.

Singh, V.P., 1989, Hydrologic systems, watershed modeling, Volume II: Englewood Cliffs, N.J., Prentice Hall, 320 p.

Swayze, L.J., 1987, Ground-water flow beneath levee 35A from Conservation Area 2B, Broward County, Florida: U.S. Geological Survey Water-Resources Investigations Report 87-4280, 22 p.

Worstell, R.V., 1976, Estimating seepage losses from canal sytems: American Society of Civil Engineers Journal of the Irrigation and Drainage Division, v. 102, no. IR1, p. 137-147.

APPENDIX I

Appendix 1. Flow measurements at L-31N Canal, March to May 1989

[Total flow is obtained from flow between transducers by applying correction factor for miles 1, 2, and 3 in table 1. AVM, acoustic velocity meter]

Date	Mile	AVM path velocity (feet per second)	Stage (feet)	Flow area (square feet)	K coefficient	Flow between transducers (cubic feet per second)	Total flow (cubic feet per second)
3-24-89	1	0.6535	4.69	1,250	0.965	789	841
	2	.6516	4.69	1,169	.995	758	805
	3	.5253	4.68	1,361	.964	689	722
3-27-89	1	.6535	4.63	1,245	.964	720	767
	2	.5827	4.62	1,164	.994	674	715
	3	.5274	4.62	1,356	.962	688	720
3-29-89	1	.6133	4.64	1,246	.964	737	785
	2	.5886	4.57	1,160	.994	679	720
	3	.4950	4.60	1,354	.962	645	675
4-3-89	1	.6131	4.65	1,247	.964	737	786
	2	.6094	4.61	1,163	.994	704	748
	3	.4655	4.61	1,355	.962	607	635
4-5-89	1	—	—	—	—	—	—
	2	.6006	4.61	1,163	.994	694	737
	3	.5107	4.58	1,352	.962	664	696
4-7-89	1	.5428	4.88	1,266	.967	665	709
	2	.5477	4.87	1,183	.998	647	687
	3	.4541	4.87	1,376	.965	603	632
4-12-89	1	.5575	4.61	1,244	.964	668	713
	2	.5352	4.59	1,161	.994	618	656
	3	.4635	4.59	1,353	.962	603	632
4-13-89	1	.5946	4.58	1,241	.963	711	758
	2	.5842	4.56	1,159	.994	673	714
	3	.4737	4.56	1,351	.962	616	645
4-17-89	1	.6288	4.70	1,251	.965	759	809
	2	.6028	4.70	1,170	.995	702	745
	3	.5255	4.70	1,362	.963	691	723
4-18-89	1	.6171	4.71	1,252	.965	746	795
	2	.5935	4.71	1,171	.995	691	734
	3	.5220	4.72	1,364	.963	686	718
4-21-89	1	.6179	4.72	1,253	.965	747	796
	2	.6155	4.73	1,172	.996	719	763
	3	.5296	4.73	1,365	.963	696	729
4-24-89	1	.6200	4.78	1,258	.966	753	803
	2	.6024	4.77	1,175	.996	705	749
	3	.5171	4.77	1,368	.964	682	714
4-25-89	1	.5598	4.65	1,247	.964	673	717
	2	.5344	4.63	1,165	.994	619	657
	3	.4578	4.63	1,357	.962	597	626
4-28-89	1	.5621	4.51	1,235	.962	668	712
	2	.5594	4.47	1,152	.992	639	678
	3	.4720	4.48	1,344	.961	610	639
5-1-89	1	.5465	4.74	1,255	.965	662	705
	2	.5447	4.76	1,175	.996	637	676
	3	.4829	4.78	1,369	.964	637	667
5-2-89	1	.5755	4.84	1,263	.966	702	748
	2	.5496	4.82	1,179	.997	646	686
	3	.4631	4.82	1,372	.964	613	642
5-4-89	1	.5356	4.75	1,255	.965	649	692
	2	.5308	4.73	1,172	.996	620	658
	3	.4354	4.73	1,365	.963	572	599
5-6-89	1	.4468	3.75	1,172	.953	499	532
	2	.4333	3.74	1,095	.983	466	495
	3	.3500	3.74	1,283	.953	428	448

APPENDIX II

Appendix II. Head measurements at L-31N Canal, March to June 1989

[Measurements shown in feet above sea level. Dashes (—) denote no data]

Date	Head at indicated sites at mile 1				
	Well 1A	Well 1B	Well 2A	Well 2B	Canal
3-23-89	4.55	4.48	4.53	4.51	4.68
3-24-89	4.58	4.60	4.55	4.55	4.69
3-27-89	4.47	4.57	4.50	4.49	4.63
3-29-89	4.41	4.52	4.46	4.46	4.64
4-3-89	4.52	4.49	4.51	4.48	4.65
4-5-89	4.50	4.45	4.47	4.48	4.62
4-7-89	4.88	4.84	4.87	4.85	4.88
4-12-89	4.54	4.48	4.53	4.52	4.61
4-13-89	4.50	4.43	4.47	4.47	4.58
4-17-89	—	—	4.62	4.63	4.70
4-18-89	4.62	4.56	4.60	4.58	4.71
4-21-89	4.72	4.68	4.69	4.71	4.72
4-24-89	4.61	4.57	4.60	4.59	4.78
4-25-89	4.51	4.47	4.52	4.51	4.65
4-28-89	4.35	4.34	4.33	4.34	4.51
5-1-89	4.70	4.67	4.69	4.70	4.74
5-2-89	4.65	4.63	4.64	4.65	4.94
5-4-89	4.50	4.46	4.50	4.51	4.75
6-6-89	—	3.49	3.55	3.56	3.75

Date	Head at indicated sites at mile 2												
	Well 3A	Well 3B	Well 4A	Well 4B	Well 4C	Well 5A	Well 5B	Well 6A	Well 6B	Well 6C	Well 7A	Well 7B	Canal
3-23-89	4.55	4.53	4.55	4.52	4.47	4.55	4.52	4.53	4.57	4.48	4.42	—	4.66
3-24-89	4.56	4.57	4.57	4.55	4.39	4.56	4.51	4.53	4.56	4.50	4.45	—	4.68
3-27-89	4.51	4.51	4.52	4.51	4.45	4.53	4.48	4.50	4.52	4.47	4.40	—	4.62
3-29-89	4.48	4.47	4.48	4.46	4.42	4.49	4.43	—	—	—	4.37	4.34	4.57
4-3-89	4.49	4.49	4.50	4.47	4.44	4.51	4.46	4.48	4.50	4.44	4.38	4.71	4.61
4-5-89	4.52	4.50	4.51	4.49	4.46	4.51	4.49	4.48	4.49	4.44	4.41	4.41	4.61
4-7-89	4.95	4.96	4.87	4.88	4.88	4.86	4.85	4.83	4.87	4.83	4.77	4.82	4.87
4-12-89	4.54	4.54	4.53	4.50	4.49	4.51	4.51	4.48	4.52	4.50	4.41	4.42	4.59
4-13-89	4.50	4.50	4.48	4.46	4.44	4.46	4.45	4.44	4.46	4.44	4.37	4.38	4.56
4-17-89	4.60	4.60	4.59	4.57	4.54	4.56	4.57	4.54	4.56	4.55	4.47	4.47	4.70
4-18-89	4.58	4.58	4.57	4.56	4.53	4.56	4.53	4.54	4.57	4.52	4.45	4.45	4.71
4-21-89	4.67	4.67	4.67	4.65	4.64	4.65	4.64	4.62	4.66	4.62	4.56	4.59	4.73
4-24-89	4.58	4.57	4.72	4.56	4.41	4.60	4.56	4.58	4.55	4.54	4.47	4.47	4.77
4-25-89	4.49	4.49	4.50	4.48	4.46	4.49	4.46	4.45	4.42	4.43	4.46	4.33	4.63
4-28-89	4.33	4.32	4.32	4.30	4.29	4.33	4.28	4.30	4.34	4.28	4.21	4.21	4.47
5-1-89	4.71	4.71	4.67	4.67	4.65	4.68	4.70	4.65	4.64	4.65	4.57	4.62	4.76
5-2-89	4.66	4.66	4.63	4.63	4.59	4.65	4.65	4.63	4.65	4.60	4.52	4.56	4.82
5-4-89	4.50	4.51	4.53	4.50	4.46	4.54	4.53	4.50	4.52	4.50	4.38	4.37	4.73
6-6-89	3.51	3.52	3.53	3.52	3.54	3.74	3.56	3.59	3.56	3.55	3.43	3.47	3.74

Date	Head at indicated sites at mile 3					
	Well 8A	Well 8B	Well 9A	Well 9B	Well 9C	Canal
3-23-89	4.57	4.42	4.49	4.39	4.40	4.66
3-24-89	4.57	4.43	4.49	4.35	4.41	4.68
3-27-89	4.54	4.39	4.45	4.35	4.35	4.62
3-29-89	4.50	4.38	4.42	4.33	4.36	4.60
4-3-89	4.51	4.38	4.34	4.36	4.36	4.61
4-5-89	4.48	4.45	4.43	4.40	—	4.58
4-7-89	4.91	4.90	4.83	4.87	4.84	4.87
4-12-89	—	—	4.45	4.43	4.40	4.59
4-13-89	4.50	4.42	4.37	4.37	4.32	4.56
4-17-89	—	5.05	4.44	4.38	4.38	4.70
4-18-89	—	—	4.49	4.44	4.42	4.72
4-21-89	4.63	4.54	4.52	4.49	4.52	4.73
4-24-89	4.61	4.49	4.53	4.47	4.45	4.77
4-25-89	4.51	4.42	4.43	4.40	4.39	4.63
4-28-89	4.34	4.26	4.29	4.25	4.22	4.48
5-1-89	4.68	4.62	4.61	4.60	—	4.78
5-2-89	4.67	4.57	4.60	4.54	4.54	4.82
5-4-89	4.56	4.45	4.48	4.44	4.45	4.73
6-6-89	3.57	3.53	3.53	3.51	3.50	3.74

APPENDIX III

Appendix III. Flow measurements at Snapper Creek Extension Canal, March to May 1989

[Positive flow is to the south; AVM, acoustic velocity meter. Dashes (—) denote no data]

Date	Station	AVM path velocity (feet per second)	Stage (feet)	Flow area (square feet)	K coefficient	Flow between transducers (cubic feet per second)
3-24-89	North	-0.01998	1.09	969	0.992	-19.2
	South	-.02816	1.08	1,955	.899	-49.5
3-29-89	North	.07090	.85	955	.985	66.7
	South	.02108	.84	1,939	.894	36.5
4-3-89	North	.04548	—	968	.992	43.7
	South	-.07999	—	1,955	.898	-140
4-7-89	North	-.01190	.93	960	.988	-11.3
	South	.00823	.91	1,944	.895	14.3
4-12-89	North	-.00938	.75	949	.982	-8.74
	South	.0051	.75	1,936	.893	8.96
4-13-89	North	-.00556	.72	947	.981	-5.17
	South	.01452	.73	1,932	.892	25.0
4-17-89	North	.00232	.95	961	.988	2.20
	South	.01347	.95	1,946	.896	23.5
4-18-89	North	-.00315	.90	958	.987	-2.97
	South	.01723	.89	1,942	.895	30.0
4-21-89	North	-.01054	.87	950	.983	-9.84
	South	-.01377	.87	1,934	.893	-23.8
4-24-89	North	-.00955	.78	951	.983	-8.92
	South	-.00613	.78	1,935	.893	-10.6
4-25-89	North	-.00798	.74	948	.982	-7.43
	South	-.00094	.73	1,932	.892	-1.6
4-28-89	North	-.01986	.68	945	.980	-18.4
	South	-.00727	.67	1,928	.891	-12.5
5-1-89	North	-.00070	.85	955	.985	- .66
	South	-.01620	.85	1,940	.894	-28.1
5-2-89	North	-.00346	.77	951	.983	-3.23
	South	-.00583	.78	1,934	.893	-10.1
5-4-89	North	-.00701	.68	945	.980	-6.49
	South	.00315	.68	1,928	.891	5.42
5-6-89	North	.00720	.32	924	.969	6.40
	South	-.01010	.30	1,904	.883	-17.0

APPENDIX IV

Appendix IV. Head measurements at Snapper Creek Extension Canal, March to June 1989

[All measurements are in feet above sea level. Dashes (—) denote no data]

Date	Head at indicated sites											
	Well 1A	Well 1B	Well 1C	Well 2A	Well 2B	Well 2C	Well 3A	Well 3B	Well 3C	Well 4A	Well 4B	Well 4C
3-24-89	0.96	0.94	0.94	0.99	0.97	0.97	0.99	1.01	1.02	1.06	1.06	1.07
3-27-89	.81	.82	.81	.82	.83	.81	.84	.83	.86	.90	.86	.91
3-29-89	.73	.73	.71	.75	.71	.73	.76	.74	.78	.82	.79	.82
4-3-89	.98	.97	.96	.97	.97	.96	.99	1.00	1.00	1.06	1.03	1.09
4-7-89	.82	.82	.79	.82	.84	.82	.83	.86	.86	.90	.88	.92
4-12-89	.63	.64	.62	.65	.66	.63	.65	—	.67	.73	.70	.74
4-13-89	.61	.60	.59	.62	.64	.61	—	—	.67	.70	.67	.71
4-17-89	.81	.79	.79	.83	.86	.82	.84	.84	.84	.93	.91	.93
4-18-89	.78	.75	.75	.79	.78	.79	.81	.84	.81	.88	.84	.90
4-21-89	.71	.73	.73	.73	.77	.78	.76	.75	.81	.84	.82	.86
4-24-89	.67	.65	.66	.65	.62	.68	.69	.71	.71	.74	.74	.77
4-25-89	.62	.63	.62	.65	.66	.62	.65	.65	.69	.70	.69	.72
4-28-89	.53	.56	.55	.58	.59	.56	.59	.59	.62	.65	.62	.66
5-1-89	.73	.70	.71	.74	.77	.73	.76	.79	.79	.82	.81	.84
5-2-89	.68	.64	.64	.68	.68	.66	.70	.71	.72	.75	.73	.76
5-4-89	.58	.56	.55	.59	.59	.56	.59	.62	.62	.62	.62	.65
6-6-89	—	.16	.17	.21	.19	.21	.21	.25	.27	.27	.23	.29

Date	Head at indicated sites											
	Well 5A	Well 5B	Well 5C	Well 6A	Well 6B	Well 6C	Well 7A	Well 7B	Well 7C	Canal N	Canal S	Canal CW
3-24-89	1.08	1.06	1.08	1.06	1.06	—	—	1.11	—	1.09	1.08	1.04
3-27-89	.89	.88	.91	.89	.88	0.86	0.92	.92	0.89	.93	.93	.88
3-29-89	.81	.81	.83	.82	.83	.78	.83	.86	—	.85	.84	.79
4-3-89	1.05	1.03	1.08	.76	1.06	1.02	1.06	1.08	1.04	—	—	1.04
4-7-89	.90	.89	.93	.89	.88	.87	.89	—	.89	.93	.91	.85
4-12-89	.71	.70	.74	.70	.74	.70	.73	.75	.72	.75	.75	.69
4-13-89	.70	.68	—	.69	.69	.67	.74	.77	.68	.72	.73	.65
4-17-89	.92	—	—	.92	—	—	.96	1.03	.91	.95	.95	.86
4-18-89	.85	—	—	.88	.89	.82	.89	.97	.86	.90	.89	.86
4-21-89	.84	.84	.86	.84	.87	.78	.87	.94	.83	.87	.87	.79
4-24-89	.73	.72	.75	.72	.75	.70	.77	.82	.73	.78	.78	.70
4-25-89	.69	.69	.71	.71	.70	.66	.74	.79	.72	.74	.73	.66
4-28-89	.64	—	.65	.63	.63	.60	.68	.70	.63	.68	.67	.64
5-1-89	.83	—	.83	.82	.83	.77	.86	.82	.83	.85	.85	.81
5-2-89	.74	—	.75	.72	.75	.69	.76	.75	.74	.77	.78	.74
5-4-89	.63	—	.65	.64	.63	.60	.64	.70	.61	.68	.68	.64
6-6-89	.26	—	.27	.27	.24	.21	—	—	.28	.32	.30	.28